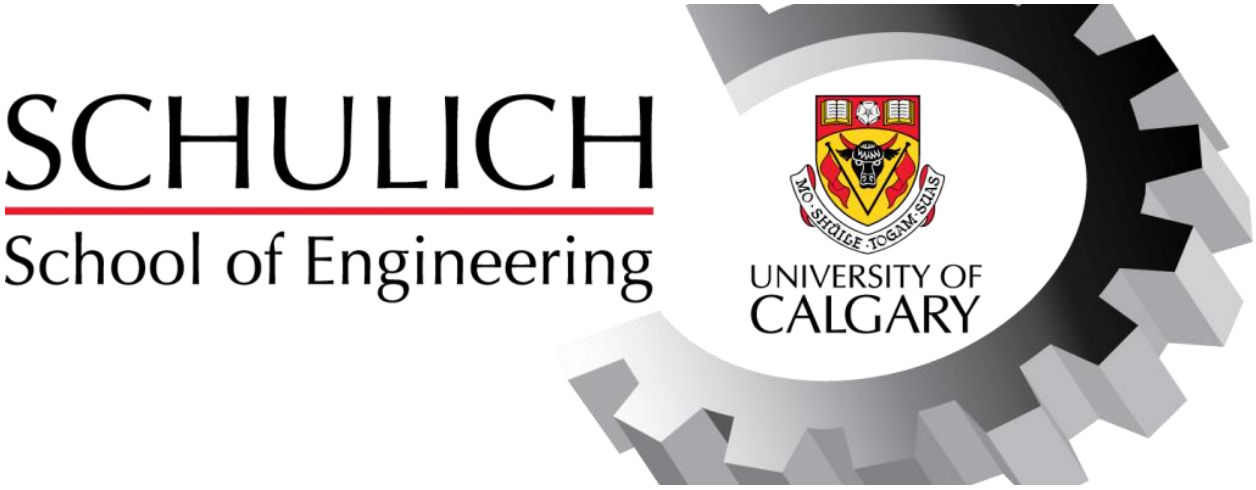

Design and Optimization of Syngas-Based Methanol Production Facility

Separation Systems and Process Intensification Strategies in Chemical Engineering Design

Authored By:

Dan Zaheer
Austin Hartwell
Alvin Ng
Kalithashinee Sivabalan
Lixin Yang

Nomenclature

BASF	Badische Anilin & Sodafabrik
BFW	Boiler Feed Water
CAGR	Compounded Annual Growth Rate
CEPCI	Chemical Engineering Plant Cost Index
CO	Carbon monoxide
CO_2	Carbon dioxide
DBM	Design Basis Memorandum
DCFRR	Discounted cash flow rate of return
D_i /D_{VD}	Inside diameter for vessel
DME	Dimethylether
G	Fluid mass flowrate
GC	Gas Chromatograph
GHG	Greenhouse Gas
GWP	Global Warming Potentials
HAZOP	Hazard and Operability Analysis
H_D	Disengagement height
H_H	Normal liquid level
H_K	Heavy key component in distillation columns
H_{LIN}	Height from high liquid level to centerline of inlet nozzle
H_{LLL}	Low liquid level height
H_{ME}	Mist eliminator
HPS	High Pressure Steam
H_S	Surge height
H_T	Total height of vessel
ICI	Imperial Chemical Industries
KT Analysis	Kepner Tregoe Analysis
LCA	Life Cycle Analysis
LK	Light key component in distillation columns
LPS	Low Pressure Steam
MAWP	Maximum Allowable Working Pressure
Mmol/h	Mega mole per hour
MPS	Medium Pressure Steam
MSA	Mass Separating Agents
MTBE	Methyl tert butyl ether
MTO	Methanol to olefins
MTPD	Metric ton per day
NPW	Net present worth
NPSHa	Net Positive Suction Head available
NRTL	Non-Random Two Liquid model

P&IDs	Piping and Instrumentation Diagrams
PFD	Process Flow Diagram
PLC	Programmable Logic Control
PRV	Pressure Relief Valves
PSA	Pressure Swing Adsorption
Q_L	Liquid volumetric flow rate
Q_V	Vapor volumetric flowrate
Re	Reynolds number
ROI	Return on investment
SMR	Steam methane reformer
Tcf	Trillion cubic feet
TCM	Thousands cubic meter
T_H	Holdup time for separators
USGC	United States Gulf Coast
U_T	Vertical terminal vapour velocity for a separator
U_V	Vapour velocity for a separator
V_H	Holdup volume
V_{LE}	Vapor-liquid equilibrium
V_S	Surge Volume
WGS	Water-Gas Shift reaction
W_s	Shaft work done by the pump
C_P°	Purchase cost
C_{BM}	Bare module equipment cost
$D_{Optimum}$	Optimum pipe diameter
D	Inner pipe diameter
H	Minimum height of liquid above the pump section
F_{BM}	Bare module cost factor
F_P	Pressure factor
f	Friction factor determined by the Moody Chart
n	Pump efficiency
P	Pressure above the liquid in the feed vessel
u	Fluid velocity
ρ	Fluid density
Δ(v)	Change in fluid velocity
Δz	Change in elevation
ΔP	Pressure difference across the pump
ΔP_f	Viscous pressure losses in the suction piping
L_{eq}	Equivalent length of the pipe
μ	Fluid dynamic viscosity

Executive Summary

An expansion of natural gas supply in North America has occurred due to the proliferation of hydraulic fracturing technology. Over the same time, there continues to be a growing demand for petrochemical derived products particularly in developing economies. This provides petrochemical manufacturers with an opportunity to turn this low-cost abundant feedstock into value-added products. Methanol's ubiquitous use as a chemical intermediate, solvent, and as a fuel additive or replacement make it an ideal product to capture this opportunity. In this report, we present a process design to turn natural gas derived syngas into 5,000 metric tonnes of methanol per day.

Our market survey revealed that there appears to be an approximately 1.65 million metric tonne per year gap between projected methanol demand and growth. The proposed design will fill that market gap. Increasing demand for petrochemical derived products will drive growth, particularly in Asia. Chinese methanol-to-olefin (MTO) technology is projected to be an important contributor to rising demand. We completed semi-quantitative analysis to determine the ideal location for this project. Our analysis indicates that the process design explored in this study would be best implemented on the United States Gulf Coast (USGC). A proposed site layout and equipment layout suitable for the USGC region are also presented.

The process design envisaged in this work is based on the Lurgi MegaMethanol™ technology currently licensed by Air Liquide. This technology was selected as it best meets our design criteria, particularly in terms of production capacity. A number of modifications were made to the aforementioned design, most notably the addition of a hydrogen pressure swing adsorption unit in order to maintain ideal reaction stoichiometry, reduce the recycle ratio from 5:1 to nearly 1:1, decrease purge stream emissions by approximately 50%, and improve process economics.

We have built on the conceptual design described in the Design Basis Memorandum submitted on December 6, 2018. We have completed our material and energy balances using Aspen HYSYS. All major equipment including compressors, pumps, reactors, and so on have undergone detailed design. The results of our detailed design are summarized in specification sheets. Design assumptions, criteria, and hand

calculations to validate our results are discussed. Hydraulic calculations and pipe sizing are summarized in tabular form. Detailed piping and instrumentation diagrams (P&IDs) for the described process are provided in addition to a process flow diagram (PFD).

Economic analyses show the proposed process is a highly lucrative venture. The return on investment (ROI) was found to be 33% with a net present value of 566 MM USD. Payback period was estimated to be 2 years. We found that process economics are most sensitive to the selling price of methanol with feedstock price and capital cost to a lesser degree.

Process safety and environmental impacts have also been considered in this work. Although the methanol synthesis process has inherent risks including flammability and toxicity, we believe these risks can be effectively managed and mitigated using proper safety controls. Preliminary HAZOP analysis was conducted to investigate engineering controls to be adopted. Possible environmental impacts of this project are described qualitatively, and greenhouse gas emissions have been quantified. Our calculations indicate that approximately 0.58 tonne of CO_2 equivalents are released per tonne of methanol produced.

By the conclusion of this report, we are confident the reader will see a promising future for methanol synthesis.

Table of Contents

List of Figures

List of Tables

1.0 Introduction

Methanol is an organic base chemical used throughout the process industries. For example, methanol is used as a feedstock to produce acetic acid, formaldehyde, dimethyl ether, and olefins to name a few. These derivatives can be used to manufacture a plethora of end products [1]. Methanol is also used as a solvent and increasingly, it is being used as a gasoline additive or alternative. Methanol synthesis was the second large-scale process involving catalysis at high pressure and temperature to be pioneered after ammonia [2]. The large-scale, industrial process was developed by Mathias Pier at Badische Anilin & Sodafabrik (BASF) in Germany [3]. Methanol is produced synthetically on an industrial scale in two steps. The first step is to convert a feedstock, typically natural gas, into synthesis gas (syngas). The second step is to convert the syngas into methanol in a methanol synthesis plant. The two principal methanol synthesis reactions are the exothermic hydrogenation of carbon monoxide (CO) and carbon dioxide (CO_2).

$$2H_2 + CO \rightleftharpoons \ CH_3OH, \ \Delta H_{298} = \ -90.8 \frac{kJ}{mol} \qquad \text{(Reaction 1)}$$

$$3H_2 + CO_2 \rightleftharpoons \ CH_3OH + H_2O, \ \Delta H_{298} = \ -49.6 \frac{kJ}{mol} \qquad \text{(Reaction 2)}$$

From the above two reactions, one can see that methanol synthesis is thermodynamically favoured at high pressure and low temperature. These methanol synthesis reactions are coupled with the water-gas shift reaction written below.

$$CO + H_2O \rightleftharpoons CO_2 + H_2, \ \Delta H_{298} = \ -41 \frac{kJ}{mol} \qquad \text{(Reaction 3)}$$

The process developed at BASF was operated at 300 atmospheres (atm) and 300-400°C using a zinc-chromite (Cr_2O_3-ZnO) catalyst [3]. Extremely high operating pressures necessitated thick-walled reaction vessels and high compression costs. A drastic step-change in process technology occurred in the 1960s when Imperial Chemical Industries (ICI) from the United Kingdom showed that methanol could be synthesized industrially at lower pressure (30-120 atm) using a copper-zinc-chromium catalyst. This technology became known as the 'low pressure methanol process.' ICI constructed and commissioned the first low pressure methanol plant in 1966 [3]. Only one high pressure methanol plant was built after 1966 [4]. It was recognized relatively early on that copper-

metal oxide catalysts were more active than zinc-chromite based catalysts, however, they were easily poisoned by sulfur impurities in the feed. Therefore, copper-based catalysts did not gain favour until advancements were made on hydrotreating catalysts to remove sulfur-bearing impurities [3].

The purpose of this work is to show that conversion of syngas into methanol using a low-pressure process is an economically attractive opportunity. The process presented herein is designed to produce 5,000 metric tons per day (MTPD) of Grade AA (≥99.85 wt%) methanol. Our design is based on the Lurgi MegaMethanol™ process currently licensed by Air Liquide [5]. Grade AA methanol is the international standard for use as a chemical building block and it may also be used as a fuel additive [6].

Lurgi methanol technologies are well-proven; Lurgi's first semi-commercial plant came online in 1970 and helped bring three plants with their technology online by 1973. Currently, Lurgi methanol technologies produced approximately one-third of the world's supply [7, 8]. There are currently fives plants worldwide using the Lurgi MegaMethanol technology, each producing approximately 5,000 MTPD [5].

For the basis of our design, we assume that an operator with expertise in syngas production is adjacent to our methanol synthesis plant and is able to deliver us high quality syngas at a competitive price. Syngas production is outside the scope of this work. It is generally believed that combined reforming, a combination of autothermal reforming and steam-methane reforming, is most economic for producing syngas at our design capacity [5, 9]. This reforming technique produces syngas with nearly perfect stoichiometric composition.

After reviewing this report, we are confident that you will see the tremendous value in methanol production using our process design. In Section 2, we will give further rationale for our selecting the Lurgi MegaMethanol™ process technology as our design basis. In Section 3, we will give an overview of the global market in terms of current and projected supply and demand. Section 4 will justify why this project should be located on the Gulf Coast of the United States. Following this, we will give a detailed description of our process and control strategies in Section 5. Detailed material and energy balances

have been completed for our process and have been summarized in Section 6. Section 7 outlines all of the detailed design completed including our design criteria and assumptions. Our economic analyses showing outstanding project profitability is discussed in Section 8. Section 9 shows our consideration of safety and environmental impacts associated with this project. This section also contains estimated greenhouse gas (GHG) emission calculations. Finally, our conclusions and recommendations are given in Section 10.

2.0 Process Selection

Several competing technologies are on the market for methanol synthesis. The primary differences between these schemes are reactor design.

A Kepner Tregoe (KT) analysis was performed to provide a comparison between reactor conditions for each process. Weighting from 1 to 5 was assigned for each criteria and a rank of 1 to 10 assigned for each process, with the higher number being more important or favourable. By taking the weightage of each criteria multiplied by the process ranking, the total for each process was obtained as a guideline to see which process would best suit our requirements.

The Slurry and Adiabatic reactors have a relatively simpler single reactor design compared to the Lurgi two reactor scheme. Multiple cold feed injection points raised the complexity of the Adiabatic reactor over the Slurry reactor. The Lurgi and Slurry reactors produced steam as a by-product, which may raise environmental concerns but can also be reclaimed to ameliorate energy requirements.

No other process could come close to the production capacity and yield of the newer Lurgi Isothermal process. The production capacity we have favored is based on the standard production rate of MegaMethanol™ plants, 5000 MTPD, which can be scaled up or down. This flexibility will allow us to size a plant with economics and design limitations in mind.

Operating at lower temperatures and pressures not only decrease safety risks but also lower equipment costs and environmental concerns. By investigating process requirements, reactants, products and by-products, we considered the adverse effect of these processes on the environment and energy requirements.

As of 2016, the most common methanol production worldwide was via the Johns-on Matthey (ICI) process which accounted for 60% of the world's methanol production. The Lurgi process came second at 27% followed up by other processes such as the Slurry reactor method [7].

As ICI was the original methanol production method since the 1960s followed by Lurgi Mega-Methanol, there has been many research papers done on these designs.

Relatively fewer studies have been conducted on the remaining processes such as Slurry and Membrane Reactors [10].

With respect to the KT analysis done, it was determined that the Lurgi Process was the most suitable for our criteria, followed by ICI while Slurry came in last. With the production capacity playing an important factor in process selection, as well as the possibility of implementing an energy recycle to further optimise the process, our group has decided to base our design on the Lurgi process involving a Steam Raising Reactor and Gas-Gas Exchanged Reactor.

Table 1 summarizes our analysis based on the order of importance for each criterion in our process selection.

Table 1: Kepner Tregoe (KT) Analysis for methanol synthesis process selection.

Criteria weighting	Criteria//Processes	Adiabatic (ICI)	Isothermal (Lurgi)	Slurry
5	Yield / Production Capacity	5 (2200 MTPD) [11]	10 (4750 MTPD) [11]	1 (237.6 MTPD) [7]
4	Process Pressure, Temperature and Safety Concerns	6 (90 bar; 224.7°C) [12]	5 (55 bar; 276.85°C) [13]	8 (52 bar; 250.3°C) [14]
4	Environmental Concerns	10	8	4
3	Energy Requirements	1	4	10
3	Operability / Complexity	6	1	10
2	Availability of information in literature	7	10	1
1	Number of industrial implementations	10	5	1
Total		134	142	116

3.0 Market Survey

Global demand for methanol is projected as 66 million tonnes annually [15]. There is a strong demand growth expected in the industry with 40% of current demand and growing is from the energy industry and for methanol to olefins (MTO) applications. Methanol is a ubiquitously produced chemical that is available globally and has chemical properties comparable to conventional fuels. Methanol is used as a reactant that enables the production of chemical derivatives which are then used to produce a vast multitude of products. Methanol is one of the most widely used industrial chemicals and is a requisite constituent for numerous chemical compounds. Primary uses are in organic synthesis, as a fuel, antifreeze, and solvents. The projected demand is expected to outpace supply as an estimated demand of a little over 3.4 million tonnes annually with a supply capacity of only 1.8 million tonnes matching this [15]. The market gap we are proposing to fill is the supply gap of about 1.65 million tonnes methanol annually. In China especially, MTO consumption is observed as a strong growing demand while growth for methanol demand for fuel is expected to continue [16, 17].

The market for methanol is segmented by feedstock, derivative, end use, industry, and region. Feedstock wise, the market is divided into natural gas, oil, coal, and renewable resources. Derivative wise, the market is compartmentalized into formaldehyde, acetic acid, dimethyl ether, gasoline, solvents, methanol to olefins (MTO), methyl tert butyl ether (MTBE) and methyl methacrylate, among others [15, 16]. The market in Asia accounts for the largest share of the methanol market. Asia Pacific is expected to account for largest market share in terms of revenue, and usage. Rapid industrialization and rising affordability of petrochemical products are strongly driving demand in China, Japan, South Korea, and India. North America is another significant market for methanol due to its ever-growing use in water treatment facilities in the denitrification process because it aids in limiting the discharge of hazardous effluents. The European market is expected to expand based on growing demand from the pharmaceutical industry with increased expenditure on healthcare and biodiesel [18].

Our proposed plant should be located near an abundant supply of natural gas. Major shale oil and gas resources exploited in Canada and the United States have

flooded the market with cheap and abundant natural gas. With strong market demand coming from the Asia Pacific region and accounting for ease of methanol transport, we investigated plant locations throughout North America. We conducted Kepner-Tregoe (KT) analysis to decide plant location. Based on our analysis, the optimal location for this plant is on the United States Gulf Coast (USGC) [19-24].

4.0 Site Selection

Several criteria were selected to evaluate the suitability of this project's location. One of the most important criterions was ensuring that the plant will have access to an abundant quantity of, preferably inexpensive, natural gas. Since natural gas is the primary feedstock for syngas production and subsequent methanol synthesis, this is absolutely critical to the long-term viability of the project. The ease of transporting our main product, methanol, and our by-product, hydrogen, were also identified as high importance criteria. Other criteria considered were tax rates, capital costs, regulatory burden, economic incentives, and overall economic viability.

Hydraulic fracturing has enabled shale gas plays throughout North America. This has led to a low cost, abundant supply of natural gas for North America's petrochemical sector. This fact coupled with the relatively stable political and regulatory climate narrowed our focus to Canada and the United States for the location of this project. Several representative regions were considered: Grande Prairie, Medicine Hat, and the Industrial Heartland in Alberta, Canada, as well as the Gulf Coast and Pennsylvania in the US.

Canada currently has a strong feedstock price advantage compared to the United States. Alberta's benchmark natural gas price, AECO, has been consistently trading at a discount compared to the United States' benchmark, Henry Hub [25]. Many point to a lack of takeaway capacity to account for the price differential [26]. Proven shale gas reserves were also explored. In Alberta, Canada, the primary shale gas formation is the Montney with proven reserves of 20.4 trillion cubic feet (Tcf) [19]. The Gulf Coast is most closely connected to the Eagleford, Permian, and Barnett shale basins with total proven reserves of 94.7 Tcf [19]. The Pennsylvania region contains the greatest proven reserves, 135.1 Tcf, locked in the Marcellus and Utica shales [20].

A number of studies have been completed comparing the attractiveness of petrochemical projects in Canada and the United States [21, 23, 24]. These studies were used to guide our analyses. These studies show that despite low feedstock prices for methanol production in Canada, considerations such as government incentives, tax rates, and market access tip the balance in favour of the US Gulf Coast (USGC).

Overall internal rate of return is approximately 2% higher on the USGC compared to Alberta and has over a 200MM USD net present value advantage [23]. The greater industrial integration on the USGC is another major advantage because it allows for simplified shipping logistics and we can sell by-product hydrogen to many nearby refineries. This conclusion is consistent with recent and current investment plans. Texas alone is expected to see 50 billion USD of investment in the petrochemical industry in the next 10 years while Alberta expects less than 5 billion in investment over the same time period [21]. Kepner-Tregoe (KT) analysis was used to definitively select the USGC as our recommended project location. The results of the analysis are tabulated in Appendix I.

5.0 Process Description

Our design is based upon our selection of the Lurgi MegaMethanol process. The process description is developed based on our PFD, which is included in Appendix A.

Syngas is taken directly from a reformer at 1008°C with a total flow rate of 32.4 Mmol/h and are separated into two flow lines for a more realistic design of pipes. Each line carries 16.2 Mmol/h of syngas. The syngas is then immediately cooled by E-100A and E-100B on each line and cooled further in E-101A and E-101B. Inlet syngas conditions were retrieved from the patent literature [27] and corroborated with simulation. Temperature control of E-100A/B is accomplished by ensuring boiler water feed is always present, while monitoring and controlling the steam output pressure [28]. The raw syngas is cooled from 1008°C to 190°C in E-100A/B by generating low pressure steam (LPS) at 177°C. The syngas then enters E-101A/B where it is cooled from 190°C to 40°C using cooling water entering the exchanger at 30°C and leaving at 35°C. These cold-water coolers are controlled by monitoring the process fluid temperature leaving the cooler and manipulating the cooling water flowrate into the cooler [28]. This significant cooling knocks out substantial water, requiring a knock-out pot, V-100, where the process water can leave for a water treatment facility. To ensure no vapor leaves from the bottom of the vessel, a liquid level is maintained within the tank by controlling liquid flow out of the bottom of the vessel [28].

24 Mmol/h syngas in the form of vapour is compressed in K-100A/B/C from a pressure of 24 bar to 100 bar. These compressors are controlled by monitoring the exit stream pressure and controlling a variable speed drive connected to K-100A/B/C compressors, which ramp the compressor up or down to meet desired pressure [28]. As the syngas heats up during compression, inter-stage heat exchangers E-102A/B/C use cooling water to cool it down to 45°C.

To achieve a stoichiometric ratio (defined in Section 6.0) of approximately 2.1, a H_2 Pressure Swing Adsorption (PSA) unit and ratio controller are used [28]. The PSA unit is made up of four beds tagged as C-100A/B/C/D. A recycle line and a purge line separated by a control valve are monitored and analyzed by the ratio controller. The ratio controller then adjusts the valve to obtain desired purge

ratio with respect to recycle flow. The H_2 rich stream leaving the PSA unit will be for sale. The H_2 lean stream is compressed by K-101 before mixed with the recycle streams (from V-102 and T-100) and PSA bypass stream, allowing us to achieve the stoichiometric ratio for our make-up syngas. Make-up syngas is pre-heated on the shell side of R-101 and then contacts catalyst in R-100. R-100 is a steam-raising, quasi-isothermal reactor with catalyst on the tube side. Our second reactor, R-101 is a gas-gas exchanged reactor also with catalyst on the tube side.

Main reactions occurring in the reactors are CO hydrogenation, CO_2 hydrogenation, and the water-gas shift (WGS) reaction. An undesired side reaction forms dimethyl ether (DME). The side reaction producing higher alcohols has been omitted from our simulation as our catalyst is more than 99% selective for our desired product, methanol [29]**.** The kinetics of all four reactions have been included in both reactors. R-100 operates at an inlet temperature of 205°C and 236°C at the exit. R-101 operates at a higher inlet temperature of 236°C and at 210°C at the exit. Both reactors give a single pass conversion of CO of 98%, CO_2 of 31%, and H_2 of 56%. Molar flow rate of 23.2 Mmol/h leaves R-101 at the reactor temperature exit. This stream composed of methanol, CO_2, CH_4 and H_2 is cooled by E-103 to 45°C before entering the flash tank, V-102.

The flash tank minimizes pressure drop before crude methanol is fed into the topping column, T-100, operating at a pressure of 6 bar. Purification of the methanol takes place in two distillation columns: the topping column, T-100, and refining column, T-101. Leaving V-102 in vapour form is mostly unreacted syngas that is recycled to increase overall conversion to product. This stream is compressed by K-102 before being recycled back into the reactors. Leaving V-102 in the liquid form is 76 mol% methanol and 16 mol% water and traces of H_2, CO_2, and DME with negligible amount of CO and N_2.

The stream then enters the topping column, T-100 at a temperature of 42°C. T-100 separates methanol and water from gases and DME. DME is set as the light key component and methanol as the heavy key component. Based on pseudo-binary system calculation, number of actual stages was set as 23, with low reflux ratio of 0.13

and reboiler duty of 24.8 MW. A partial condenser was used for this column. To prevent overheating, temperature is regulated by controlling valve allowing liquid reflux to be pumped back into top of the column [28]. Liquid level in the column is also maintained using a level transmitter which controls a valve on the bottoms line leaving the column [28]. DME with a recovery of 99% leaves as distillate from T-100. This stream contains DME and traces of syngas and is compressed by a multi-stage compressor, K-103A/B/C, before recycled back into the reaction system. A stream of 0.828 mole fraction of methanol and 0.172 mole fraction of water leaves as bottoms product from T-100. This stream is pumped to high pressure to prevent vaporization and pre-heated in E-107 with medium pressure steam. It is then sent through an expansion valve to drop the pressure to 1.8 bar, generating a 50/50 mixture of vapor and liquid. The methanol and water separation is accomplished in the refining column, T-101.

The stream enters the refining column, T-101 at a temperature of 84°C. The refining column, T-101 operates at a pressure of 1.8 bar and separates methanol and water. This is a binary system with methanol as the light key component and water as the heavy key component. Based on our calculations from theoretical number of stages, number of actual stages were set at 36, with a reflux ratio of 1.352 and reboiler duty of 160 MW. A total condenser was used for this column. Methanol recovery of 99% with purity of over 99.85 wt% was achieved. Further details on the column duties can be referred to in Appendix B.

The methanol product stream leaves from top of the column as distillate at a temperature of 67°C. Process water leaves as bottoms product with a mole fraction of 0.9536 water and 0.0464 mole fraction methanol at a temperature of 105°C. This stream goes to water treatment facility while the grade AA methanol stream is cooled through E-110 to 40°C before sent to storage tanks. We achieved our design objective with production of 5075 metric ton per day methanol with a purity of over 99.85 wt%.

5.1 Control Strategies

The process flow within a system is always assumed to be within an expected range and condition set from the controls upstream. With this assumption, we can be certain that processes generally stay within operable conditions and capabilities of the units. Safety precautions are in place which should prevent over pressuring and initiate emergency shutdowns if required [28].

COOLERS:

Waste Heat Boilers: E-100A, E-100B

Boiler feed water is water that has been treated to prevent corrosion, scaling or foaming within the system during boiling or cooling. Waste heat boilers use boiler feed water to absorb heat energy from a process stream, by evaporating the boiler feed water into steam. This steam can then be used as an energy source, depending on the desired set pressure. Temperature control of this type of cooler is controlled by ensuring boiler feed water is always at an adequate level to submerge the tubes, while monitoring and controlling the steam output pressure. This is done by a level transmitter which controls the boiler feed water valve, while the steam output pressure control is done by regulating a valve on the steam line after the pressure sensor, generally on the top of the cooler.

Cold Water Cooler: E-101A/B, E-102A/B/C, E-103, E-106A/B, E-110

Cold water coolers or heat exchangers use cold utility water to cool a process fluid. It is controlled by monitoring the process fluid temperature leaving the cooler and manipulating the cooling water flowrate into the cooler to obtain the target process temperature. This allows for minimal time delay and greater response or effect on the process fluid temperature when opening or closing the valve. The input of the cooling water is towards the process exit end of the cooler to ensure that the leaving fluid has the highest cooling priority.

Partial / Total Condenser: E-104, E-108

Condensers are not only used to either condense out components from the vapor stream, or fully condense the vapor stream, but to also maintain pressures within the distillation column. By monitoring the pressure of the line leaving the top of the distillation column and controlling the cooling water flow into the condenser, condensers control the pressures directly and regulate temperatures indirectly.

HEATERS:

Topping / Refining Column Reboiler: E-105 / E-109

Distillation columns reboilers are used to maintain the required bottoms elevated temperatures. They are controlled by monitoring the distillation column bottoms temperature and controlling the steam flow into the reboiler, which heats the boil up and in turn increases the bottoms temperature. The process liquid level is regulated in the column, which in turn ensures that the reboilers are always flooded.

Refining Column Feed Exchanger: E-107

This shell and tube heat exchanger utilizes medium pressure steam as an energy source to heat up the topping column boil up, before it is processed in the refining column. Steam flow into the shell side is controlled by monitoring the exiting process fluid temperature in the tube side. This is then used to control a valve controlling the flowrate of the entering steam on the process exit end of the exchanger, to ensure that the leaving fluid has the highest heating priority and the heating adjustment has the shortest time delay.

VESSELS:

Two Phase Separators: V-100, V-101A/B/C, V-102, V-104A/B and Reflux Vessels: V-103, V-105

Two phase separators are maintained at a steady state pressure to control the vapor composition leaving the vessel. Pressures within the unit are controlled by a pressure transmitter is located on the top vent line followed by the control valve. To ensure no vapors can leave from the bottom of the vessel, a liquid level is maintained within the

tank by monitoring the tank liquid level while controlling the liquid flow out from the bottom of the vessel. In the case where the vessel is located on the reflux line of the Topping or Refining column, since the pressures is regulated by the condenser between the column and vessel, only liquid level regulation is required.

Topping / Refining Column: T-100 / T-101

The condenser and reboiler on the top and bottom of the distillation tower not only help to control the temperatures in their respective regions of the tower, but pressures as well. Temperature transmitters and control systems are installed on the top and bottom of the column to control liquid reflux from the condenser being pumped back into the top of the tower and steam being fed into the reboiler at the bottom. This ensures no overheating occurs at the top of the tower, as well adequate boil up temperatures at the bottom of the tower. To maintain a set liquid level within the column, a level transmitter and alarm system is installed to control a valve which regulates the bottoms product leaving the system. Lastly a pressure control system is installed on the top of the column which regulates the downstream condenser.

COMPRESSORS:

Syngas Compressors: K-100A/B/C, K-101, K-102, K-103A/B/C

Compressors are controlled by monitoring the temperatures, pressures and flow of the process vapors entering and leaving the unit. This information would then be fed to a programmable logic control (PLC or DCS), connected to control valve on a recycle loop. Theoretically this configuration should not only prevent anti surge but would also ensure that the compressors reach the required outlet pressures. However, as this technology is usually proprietary information, we would require compressor vendor confirmation.

REACTOR:

Steam Raising Reactor: R-100

Normal Operating Conditions:

Under normal operating conditions, boiler feed water is sent to the bottom of the reactor on the shell side. Methanol synthesis is an exothermic process so steam is generated to cool the reaction. Level control is used to ensure boiler feed water always covers the tubes. The steam pressure leaving the shell side is controlled using a valve on the MPS outlet. The steam raising reactor is unique because the pressure of the heat transfer fluid (the steam being raised) changes its temperature. This is because the boiler feed water and steam exist as a single component, two phase mixture. This means there is only one thermodynamic degree of freedom. The temperature of the steam, in turn, affects the temperature of the reacting syngas on the tube side. We decided to implement cascade control on this reactor. The primary controller is the temperature controller for the reaction mixture while the secondary (slave) controller adjusts the steam pressure. Under our designed steady-state conditions, the reactor temperature will be held at the optimal temperature while producing on-spec medium pressure steam. A differential pressure indicator should be installed to measure the pressure drop through the catalyst bed as the plant run evolves.

Start-up Conditions:

During start-up, medium pressure steam is provided to the reactor instead of boiler feed water until the reactor is brought up to temperature. As the reactor warms up, steam will condense on the tubes and will be withdrawn from the BFW return line. As steam is slowly added, the observed temperature of the syngas entering R-100 will slowly start to rise as the exothermic reaction occurs at higher rates and heat is exchanged in the gas-gas exchanged reactor. Once the desired R-100 syngas feed temperature is achieved, the steam supply line and BFW return line will be closed. The boiler feed water supply and medium pressure steam header return lines will be opened simultaneously to begin normal operation.

VALVES:

Ratio Controllers: VLV-120, VLV-149 above V-102 and V-155 above V-103

Ratio controllers are used in the system to consistently purge a required percentage of the recycle stream. To accomplish this, a recycle line and purge line is separated by a control valve. The flows of the recycle and purge lines are both monitored and analyzed by a ratio controller which adjusts the valve to obtain the desired purge ratio with respect to the process flow.

COLUMNS:

Pressure Swing Adsorption (PSA) Units: C-100A/B/C/D

The pressure swing adsorption unit utilizes alternating pressures and an adsorbent bed of Zeolite 5A and Activated Carbon to remove H_2 from our feed syngas. Under high pressure, syngas components other than H_2 are adsorbed to the bed. Under low pressure, these components are desorbed to regenerate the bed. The H_2 deficient syngas is sent for further processing to adjust the stoichiometric module. Each bed goes through the following stages each cycle:

1. Adsorption
2. Depressurization
3. Regeneration
4. Repressurization

Although this process is inherently unsteady, multiple beds in parallel allow the process to continuously perform the separation. The length of time for each of these stages is programmed and depends on the operating conditions and size of the beds. The next stage for each bed will occur after a specified amount of time has elapsed. Certain valves must be rapidly fully opened or fully closed at the specified time for each stage to proceed successfully. Figure 1 of the time dependent control strategy is attached below, and this is controlled by an intricate series of valves and pipelines as shown in the P&ID. The valves are controlled by a PLC, programmed to follow the timed process, while also monitoring the differential pressures across the beds to ensure the process is continuing as expected and the adsorbent bed is active [30]. As a precaution an alarm on the PLC is added to notify the operator during upsets and a GC is setup to monitor the quality of the H_2 product stream.

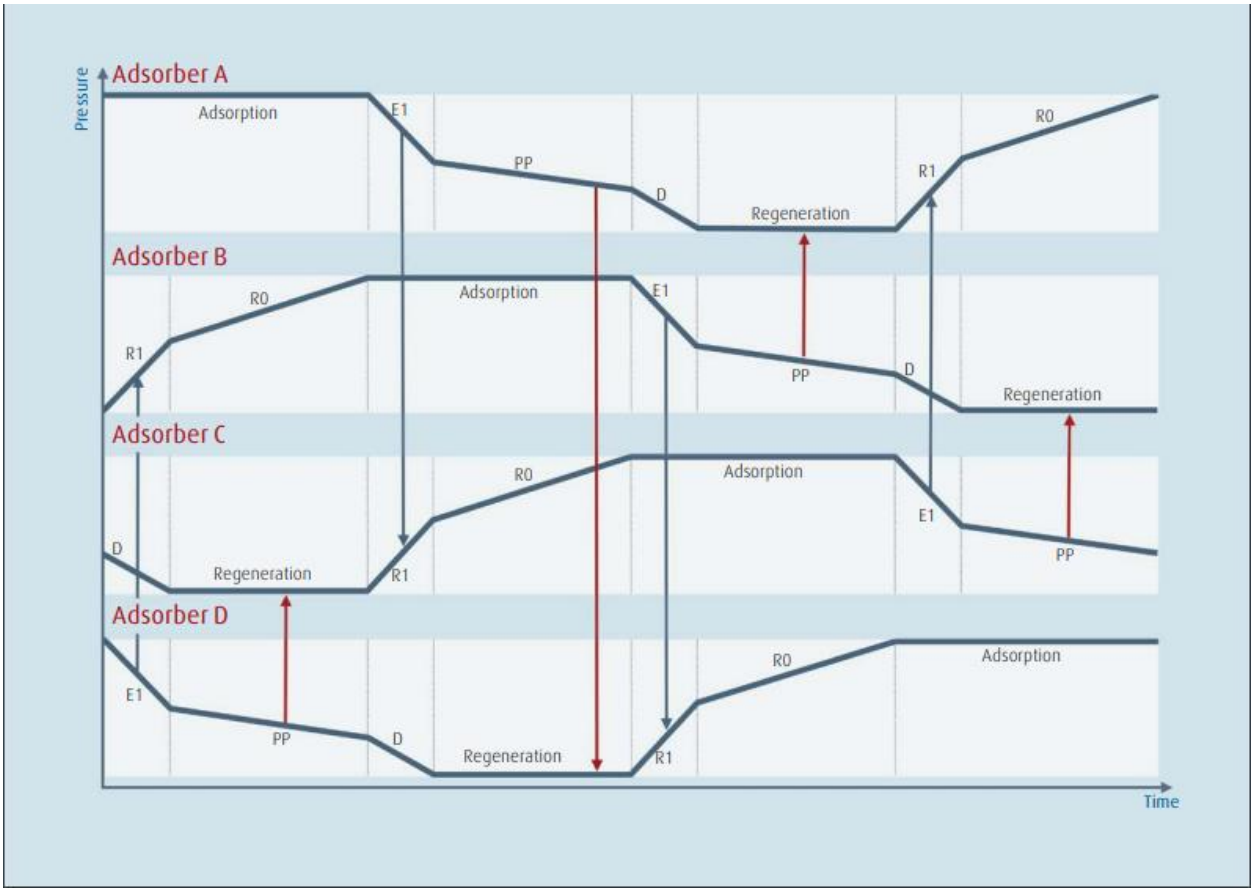

Figure 1: PSA Controls Cycle.

6.0 Material and Energy Balances

Material and energy balances have been completed using Aspen HYSYS. Please refer to Appendix B for the complete Material and Energy balance table. Our thermodynamic package selections have also been validated against experimental data. Thermodynamic package verification was discussed in the Design Basis Memorandum (DBM).

Syngas is differentiated based on its stoichiometric ratio of components. The stoichiometric ratio is characterized via the module, M, defined as follows:

$$M = (n_{H_2} - n_{CO_2})/(n_{CO} + n_{CO_2}) \quad \text{(Equation 1)}$$

Where n_j is the number of moles of component j. For methanol synthesis, the ideal module is between 2.05 and 2.10 for syngas with impurities [31]. While detailed design of the reforming section was not in the scope of the current work, we did simulate the combined reforming process in Aspen HYSYS using Gibbs (equilibrium) reactors. Since reforming reactors are generally equilibrium limited, this yields a simulation representative of more in-depth study. In this way we were able to verify the syngas composition and conditions being fed into the methanol synthesis plant. It was also done to quantify the amount of steam, natural gas, and oxygen required to produce nearly optimum syngas for methanol synthesis [31]. For the MegaMethanol™ technology, combined reforming is typically employed to generate the syngas [8]. In combined reforming, an oxygen-blown autothermal reformer is used in concert with a conventional steam methane reformer (SMR). Autothermal reforming alone produces syngas with a stoichiometric module less than 2, while a SMR alone produces the same with a module much greater than 2. The exit temperature of the autothermal reformer is typically between 950 and 1050°C [8, 27]. The composition, temperature, and pressure of the simulation we obtained are very close to that described in the patent literature [27]. The temperature of the autothermal reformer outlet was found to be 1008°C in our simulation. Our simulated combined reforming process generated syngas with a module of 2.1.

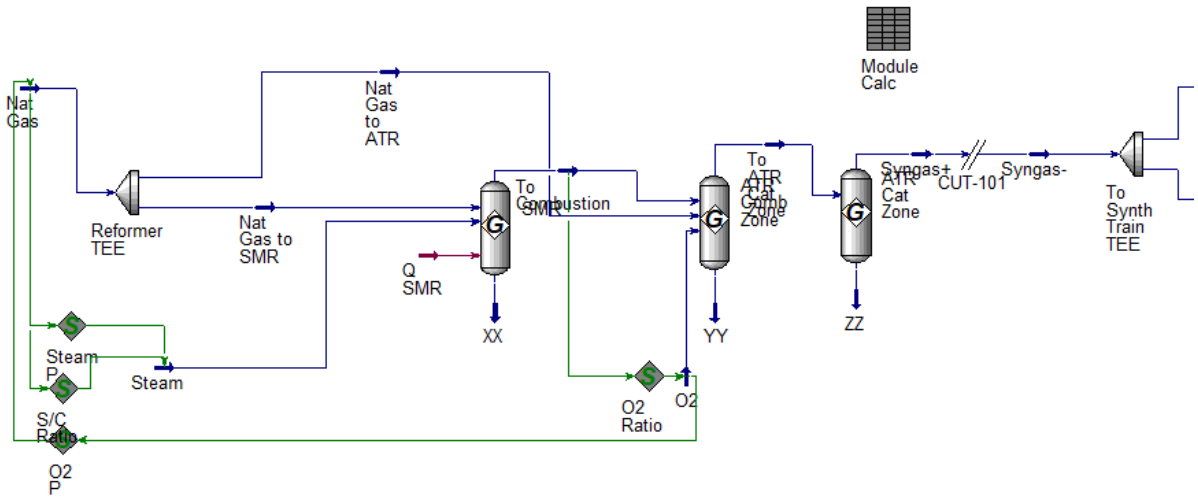

Figure 2: Aspen HYSYS screenshot of reforming section.

Despite the fact that nearly ideal stoichiometric syngas can be produced using combined reforming, relatively small quantities of hydrogen among other components can accumulate in the synthesis recycle loop. In order to ensure ideal module syngas is consistently fed into the synthesis reactor system, the hydrogen content can be adjusted. Hydrogen is commonly purified from syngas streams using PSA units. The effect of diverting a portion of fresh syngas to a PSA unit is shown in Figure 3 below.

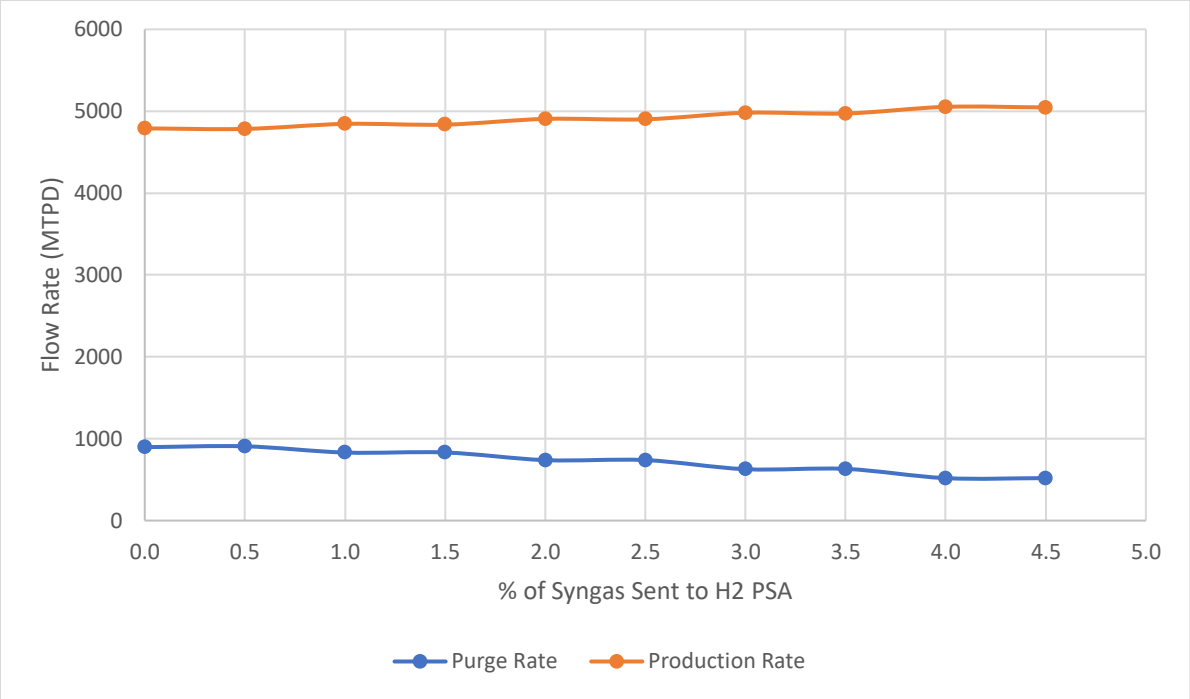

Figure 3: Recycle purge rate and methanol product flow rate versus percentage of fresh syngas sent to PSA unit at constant stoichiometric module.

As the figure demonstrates, the methanol production rate can be increased while decreasing purge rate at an ideal stoichiometric module. This requires no additional syngas feed. As an added benefit, we are able to generate high value, pure hydrogen. Further syngas sent to the H_2 PSA unit leads to unstable numerical solution in Aspen HYSYS. Therefore, ~4% syngas diversion appears to be ideal for the fresh syngas composition in this work. This process modification minimizes environmental impacts by decreasing the purge rate to flare while improving economic performance. An added benefit of this is addition is greater operational flexibility. Our process can tolerate variations in syngas composition more effectively than the standard MegaMethanol™ system. Aspen HYSYS does not have a unit to rigorously model PSA units. Therefore, a component splitter was used to simulate the PSA in the flowsheet. Detailed PSA design is described in Section 7.3. Since H_2 lean syngas is produced from the PSA unit during the desorption phase, it is only available at low pressure (approximately 2 bara). This led to an interesting problem: how do we get the H_2 lean syngas up to reaction pressure without drastically increasing capital and operating compression costs? We found that a single stage compressor can be used if the H_2 lean syngas stream is tied into the recycle

stream originating from the topping column. We also considered creating another recycle loop and mixing the H_2 lean syngas with the fresh inlet syngas. However, a multi-stage compressor would be required to overcome the adverse pressure gradient. Our design decision to implement K-101 in this fashion prevented the addition of another multi-stage compressor and allowed us to simply modify equipment already designed.

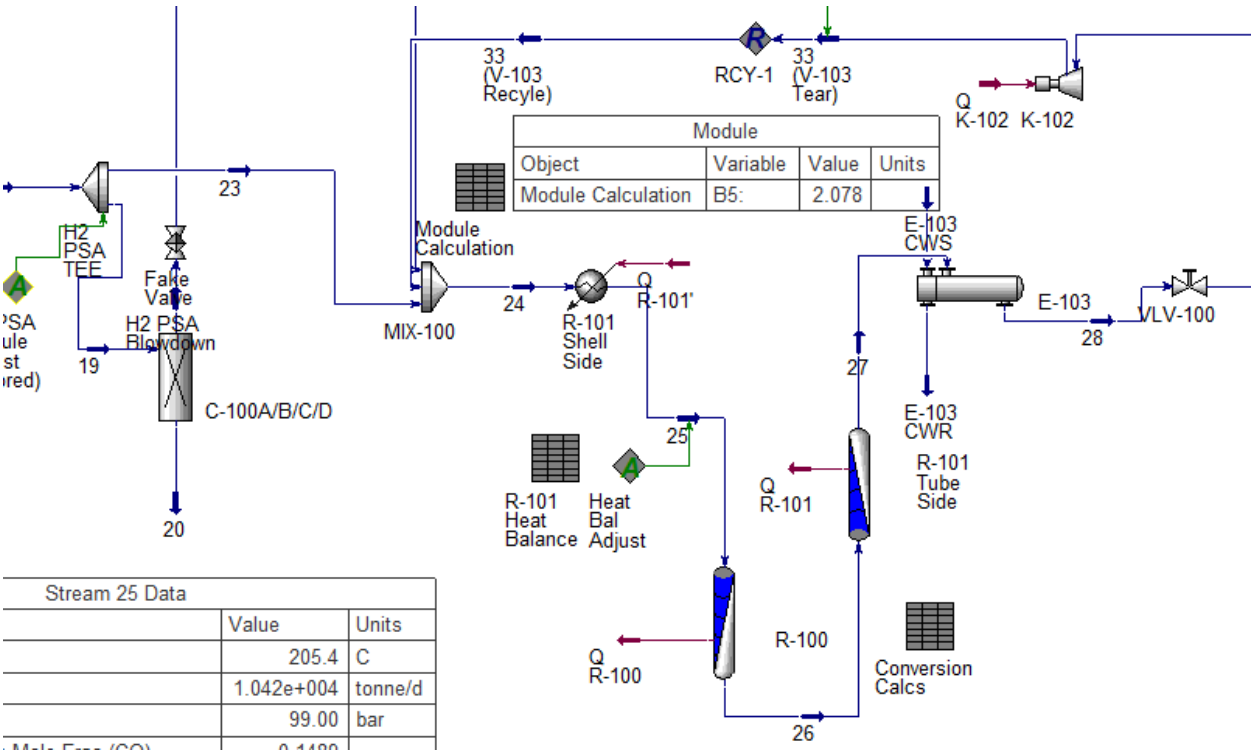

Figure 4: Aspen HYSYS screenshot of PSA and methanol synthesis section.

When we began simulations, we found that large quantities of methane (CH_4) accumulated in the syngas recycle stream. This is because methane is not consumed nor produced in the reaction system. Methane can be thought of as an inert material in the context of methanol synthesis. We investigated the feasibility of implementing a Pressure Swing Adsorption (PSA) unit to remove the CH_4 from the feed stream. However, preliminary sizing indicated that an extremely large quantity of adsorbent and numerous PSA beds in parallel would be required to treat the syngas feed stream. In addition, it was found that common adsorbents for CH_4 may have deleterious effects on the syngas

composition. Therefore, we decided to forgo adsorption for the purpose of removing methane.

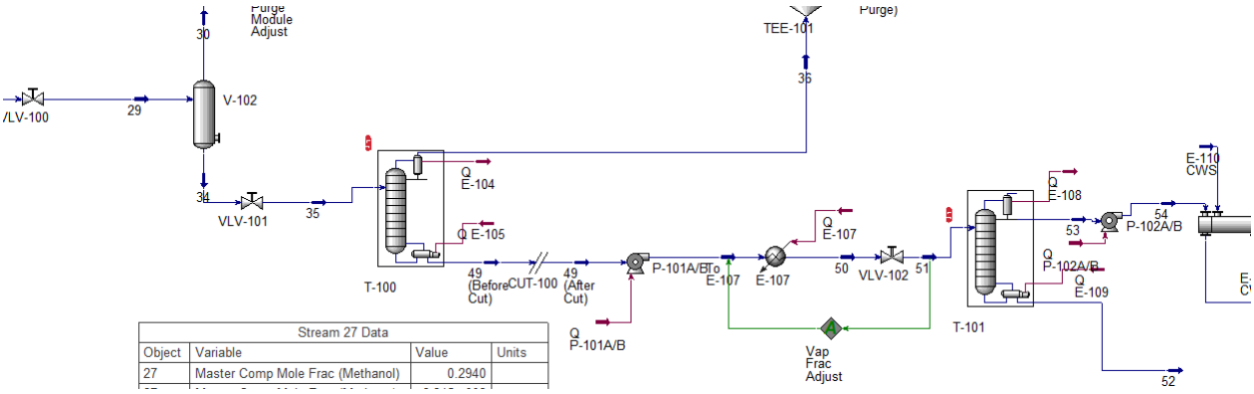

Figure 5: Aspen HYSYS screenshot of product purification section.

The effect of reactor pre-heat temperatures on reactor temperature profiles, plant productivity, and so on was extensively studied. It was found that increasing the pre-heat temperature into the steam-raising reactor (R-100) has a significant impact on plant performance. We found that higher plant productivity can be achieved by increasing pre-heat temperature and producing medium pressure steam instead of high pressure steam typical of Lurgi synthesis reactor systems.

Increases in R-100 pre-heat temperature correspond to decreases in R-101 effluent temperatures due to the heat exchanged nature of R-101. Lower operating temperatures at the outlet of R-101 are favourable from a thermodynamic perspective. See Figure 6 below. Therefore, higher conversion to methanol can be achieved. In order to counter-act the increased feed temperature to R-100, the steam raised by R-100 must be generated at a lower temperature. The temperature in both reactors is limited to approximately 300°C because higher temperatures are known to significantly sinter the copper-based catalyst [32]. Typically, the steam-raising reactor in the Lurgi MegaMethanol™ process generates high pressure steam. In our design, the steam-raising reactor is modified to produce medium pressure steam.

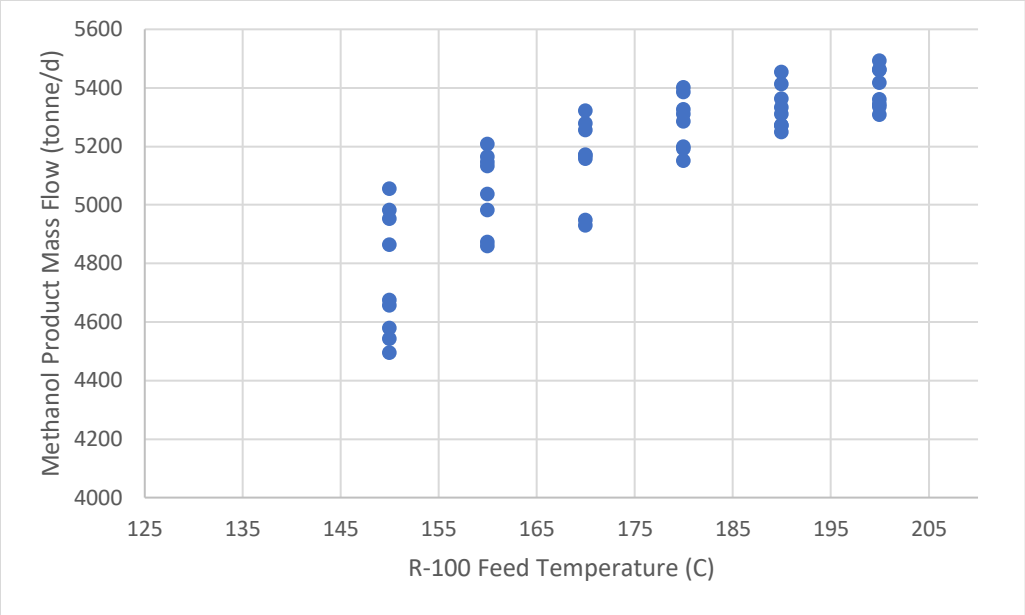

Figure 6: The effect of steam-raising reactor (R-100) feed pre-heat temperature on process productivity.

During the simulation, it was found that lowering the reaction pressure slows the reaction as expected. Decreasing pressure decreases the fugacity of the reactants and decreases the rate of reaction. If excessive sintering of the catalyst pellets is noticed after installation, we recommend decreasing the reaction pressure. This way, the maximum temperature in the beds decreases thus prolonging catalyst life. This has the added benefit of decreasing the compression costs incrementally.

7.0 Equipment Sizing and Detailed Design

7.1 Material Selection

Material selection is not only important to ensure no material failures will occur during the lifespan of the project, but to accurately estimate capital costs, and ensure the safety of personnel and the general public. A direct weighting method was used in the material selection process. It was done by identifying the components and process conditions of concern within our system [33].

The components of major concern with respect to corrosion within our system were hydrogen gas, water, carbon dioxide and methanol.

Hydrogen is a major concern due to embrittlement occurring when hydrogen under high pressures readily diffuses into the metal lattice structures and accumulates at the grain boundaries. Simply by the accumulation or reaction of hydrogen with the metal, it can weaken the material strength, leading to fractures [34].

Water and CO_2 are a concern because when combined, lowers the pH of water by forming carbonic acid which promotes metal corrosion. Water with naturally dissolved minerals or ions causes it to become a good oxidizer, which corrodes and weakens metals with the formation of oxides or rust. Even oxygen from the air being dissolved in the water causes the severest form of pitting corrosion [34].

Methanol was the last concern due to the fact that it would be our major product and with high concentrations and flow of the material, even a little corrosiveness would be amplified in the product stream.

Next, we identified the concerning process conditions within our simulation and coupled them with the major components of concern. From the feed stream to V-100 (water knock out drum), water along with high temperatures of over 1000^{o}C until after the coolers were deemed a major concern. Thus, following the guidelines for using Stainless Steel in Water industries, due to no chlorine content and including a safety margin, 316 SS was selected over 304 SS for that section [35].

With water now almost completely removed from the system and temperatures below 242^{o}C, a new material selection process could be done by re-evaluating the process conditions and components.

Between the V-100 water knock out pot and R-100, R-101 reactors, hydrogen is at a maximum temperature of 150^{o}C. Thus, the API general material selection recommends Carbon Steel [33].

For the R-100 the Gas-Gas Exchanged Reactor and R-101 Steam Raising reactor, due to the increased temperatures of 242^{o}C and pressures of approximately 100 bar, a more stringent standard was selected to be implemented. The American Petroleum Institute standard 941: Steels for Hydrogen Service at Elevated Temperatures and Pressures in Petroleum Refineries and Petrochemical Plans was referenced [33]. By determining the hydrogen partial pressures and maximum process temperature, Figure 7 (see below) was referenced and the material most compatible for the following process was a steel alloy of Tempered Fe-Cr-Mo Alloy (Code 1211) [33, 36].

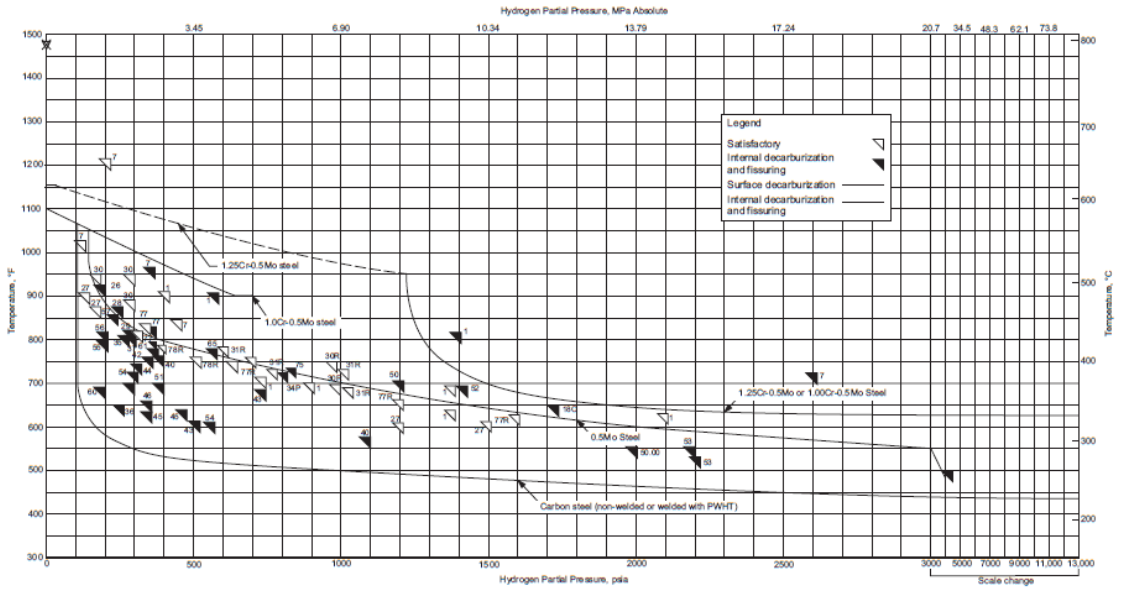

NOTE 1 References and comments are shown on Table A.1.
NOTE 2 Curves for carbon steel, 1.0Cr-0.5Mo steel, and 1.25 Cr-0.5Mo steel are included for reference.
NOTE 3 The symbol ◹ is retained as a reference against previous editions of this publication.
NOTE 4 Reference numbers are the same as in previous editions of this publication.
NOTE 5 The 0.5Mo steel curve is the same as the one shown in the Seventh Edition of this publication (2008).

This figure was revised by API in 1969, 1983, 1990, 1996, and 2015.

Figure A.1—Experience with C-0.5Mo and Mn-0.5Mo Steel in High Temperature Hydrogen Service

Figure 7: Nelson curves from API Recommended Practice 941.

After the reactors, temperatures and pressures within the system follow the trend of the system between V-100 and the reactors. Thus, according to the API standard Carbon Steel is adequate. Now considering methanol, which is only present after the reactors, we referenced the methanol institute guidelines for neat methanol service to confirm that Carbon Steel is suitable for the process conditions [37].

Line sizing and specifications where done next to confirm that piping in that specific material was not only available in the required size but would be able to handle the operating pressures and temperatures.

Galvanic corrosion is a chemical process which occurs when different metal comes into contact, leading one metal corrode preferentially over the other. Although simple solutions, such as using insulative gaskets between piping can be a solution, the potential

risks can be significant and increase associated costs; thus the selection of differential metals was done conservatively.

Material selection of existing plants with similar process conditions were also referenced to ensure that our selection was not only theoretically sound, but so that the estimated costing of the project would be more accurate.

7.2 Reactor Design

The reactor design was based on the kinetics reported by Park et. al. using a three-site adsorption model [38]. The commercial catalyst used in this study was a Cu/ZnO/Al-$_2O_3$ based Clariant/Süd-Chemie MegaMax 700. This study was selected because Clariant's catalysts are used in the MegaMethanol™ system [39]. Dimethyl ether (DME) formation was also considered. Other side reactions were neglected as methanol synthesis selectivity of 99.9% is not uncommon [40]. Park used Ng et. al.'s formulation for DME formation kinetics and we used them in this work as well [38, 41]. Park et. al. based their kinetic model on the knowledge of which elementary steps are rate limiting as determined by Graaf et. al. [42]. The work by Graaf et. al. was consulted to find equilibrium constants when they were not given by Park et. al.

The internal mass transfer limitations of the commercial catalyst pellets cannot be ignored. Park et al. showed that the effectiveness factor for a full-size catalyst particle is approximately 50% [38]. This was taken to be representative of our system and was applied to our reactor design. External mass transfer limitations were ignored for this work as the flow through the tubes was established to be turbulent ($Re > 10^4$). Furthermore, plug flow was assumed; axial dispersion and other effects such as channeling were neglected.

Heat balance of the gas-gas exchanged reactor was found to be a formidable task. In order to simulate the heat transfer of the gas-gas exchanged reactor (R-101), heat transfer parameters representative of the cool syngas were input into the HYSYS reactor model. These heat transfer parameters had various effects on the downstream process so we had to adjust parameters iteratively to achieve convergence. We were able to

demonstrate that the gas-gas exchanged reactor works as designed in the simulation. The error of the heat balance in HYSYS is within 10%. This is more than acceptable given the relatively high uncertainty in the correlations used to calculate heat transfer coefficients.

We initially expected to produce low pressure steam from the steam-raising reactor, R-100. However, this model did not account for internal mass transfer limitations causing a lower apparent rate of reaction. It was found that the lower apparent rate could be partially counteracted by using a higher temperature heat transfer medium (i.e. raising medium pressure steam instead).

The catalyst pellets were assumed to be 6mm x 5mm. This is one of the catalyst sizes offered by Clariant [43]. Sphericity and equivalent particle diameter were calculated. A bed void fraction of 0.4, typical of random packing was selected. The Ergun equation was used to calculate the pressure drop across each bed. Detailed reactor specifications including dimensions are given in Appendix D: Equipment Specification Sheets. The sample calculation for reactor sizing is still applicable from the Design Basis Memorandum (DBM) given the simplifying assumptions associated with it such as using partial pressures instead of fugacities. The reactor temperature profiles are given below:

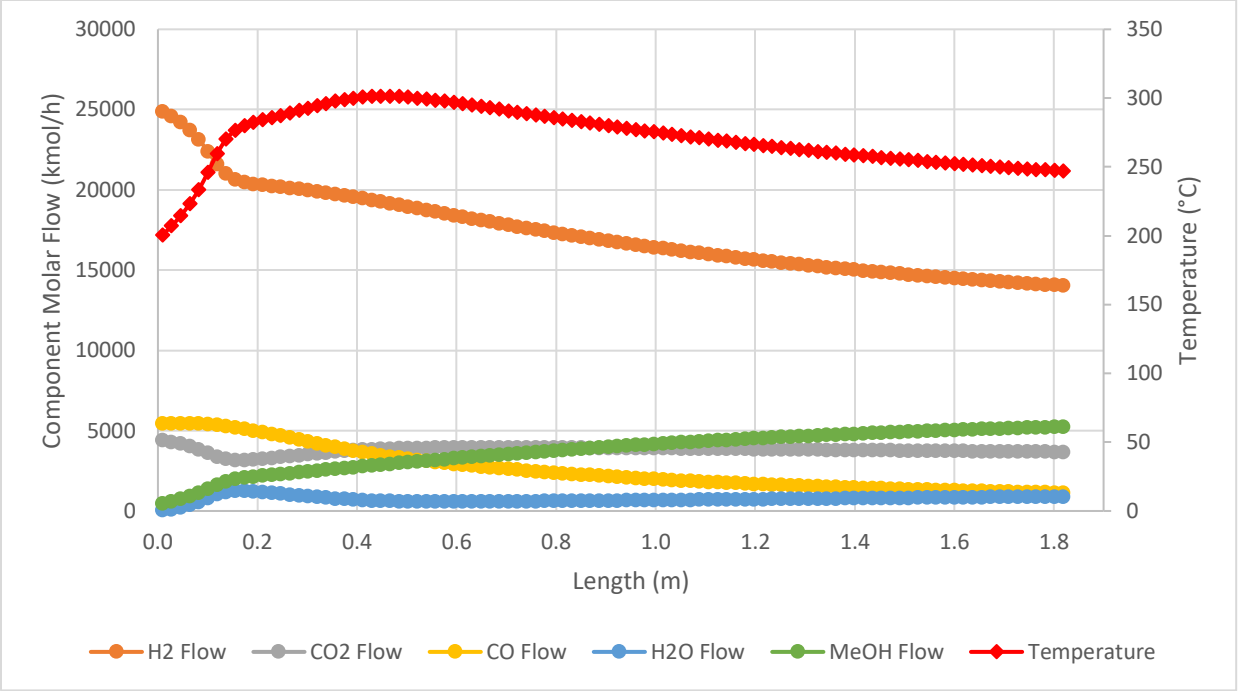

Figure 8: Temperature and composition profiles of the steam-raising reactor, R-100.

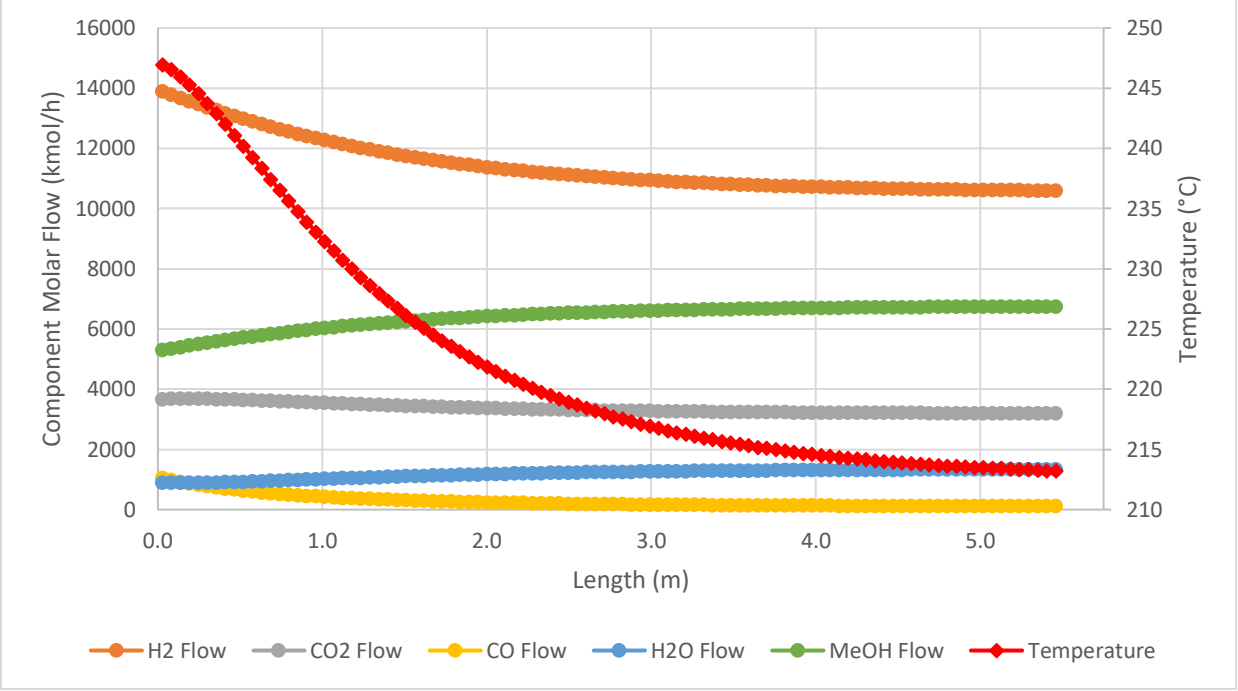

Figure 9: Temperature and composition profiles of the gas-gas exchanged reactor, R-101.

7.3 Pressure Swing Adsorption (PSA) Design

Pressure Swing Adsorption (PSA) units cannot be rigorously modelled using Aspen HYSYS. In order to simulate the PSA unit in Aspen HYSYS, a component splitter was employed. Despite advances in modelling pressure swing adsorption units, detailed design of PSA units still remains largely an experimental endeavour [44, 45]. The separation of H_2 from syngas is also inherently complex because it is non-dilute, multicomponent, unsteady state, non-isobaric, and non-isothermal. In addition, the boundary conditions vary during start-up.

In this process, H_2 quickly breaks through the bed while the other syngas components are adsorbed. We decided to base our PSA unit around a four bed system with a cycle based on Linde's hydrogen recovery technology [29]. A four bed PSA unit was pioneered by Union Carbide [46]. A hydrogen recovery rate of 75% and hydrogen product purity of 100% were assumed. This hydrogen product purity is reasonable because PSA units routinely deliver hydrogen with >99.9% purity in industry [47]. A recovery of 75% is also consistent with typical operation of a modern four bed system [48].

Conservative hand calculations were used to ascertain the amount of adsorbents required and thus size the beds. We selected Zeolite 5A and activated carbon as our adsorbents. These materials are typically layered in a single vessel for the separation of H_2 from syngas [47]. Activated carbon is preferred for the adsorption of CO_2, while Zeolite 5A is preferred for the adsorption of CO and N_2. Both Zeolite 5A and Activated Carbon can be used to remove CH_4 [47]. In refineries, a layer of silica gel is typically used to adsorb C_3+ compounds but they are not present in our syngas, so this layer was omitted from our design. The diameter of the adsorption beds must be selected such that the superficial gas velocity through the bed is acceptable. A superficial velocity between 0.01 and 0.05 m/s has been suggested in the literature [49]. An adsorption time of 400 second (1600s total cycle time), was selected as it gave a reasonable adsorber size. This is a justifiable adsorption time because complete cycle times are typically on the order of 10 minutes [50]. Cycle times are typically limited by hydrodynamics when rapidly de-pressurizing the beds.

H_2 PSA units are based on equilibrium adsorption selectivity [51]. Adsorption capacity was calculated based on the competitive adsorption isotherms given by Yavary et. al. [52]. Yavary et. al. showed that the isotherms are well fit to a Langmuir model. It should be noted that the Langmuir isotherm had to be extrapolated to our operating pressure due to a lack of additional data. To ensure that our beds were conservatively sized, we assumed an adsorbent utilization of 65% as suggested in the literature [49]. This corresponds to an ideal (flat) mass transfer front reaching 65% of the way through the bed before adsorption is switched to another bed. Pressure drop through the bed was calculated using the Ergun equation with adsorbent particle sizes typical in industry. Sample calculations are provided in Appendix J.

The dimensions, details of the adsorbents selected, and cycle data is provided in Appendix D.

7.4 Distillation Column Design

Distillation columns are essential for separation of final products from unwanted impurities. Distillation was chosen as our main separation process because it has relatively high mass transfer rate and the process is flexible for scaling. It is also a very reliable separation design and relatively cheaper than Mass Separating Agents (MSA) such as liquid-liquid extraction or adsorption processes [53].

A KT analysis was performed in the selection of type of tower that would be suitable for our design. Based on the analysis presented in Table 2, sieve tray design was selected for our two distillation columns, T-100 and T-101. Based on our hand calculation performed for Design Basis Memorandum (DBM) last term, we determined our distillation columns will have large diameters. Sieve tray columns would be more capable to handle the pressure drop through the column and is more cost effective for large diameters [53]. As our component to be separated includes water that could initiate corrosion, sieve tray is a good choice as it has high resistance to corrosion.

Table 2: Distillation tower internal design type selection

Criterion	Criterion Importance Multiplier	*Bubble Cap*	*Sieve*	*Valve*
Capacity	1	2	3	3
Efficiency	2	2	3	3
Maintenance	2	1	3	2
Turndown	1	3	2	2
Cost	3	1	3	2
TOTAL	-	**14**	**26**	**16**

The detailed design of the distillation columns was done using KG Tower. Tray pass of four was selected for more efficient liquid distribution in the topping column, T-100. Two tray passes were used in the design of the refining column, T-101 as design with more passes faces issue of jet flooding due to excessive froth entrainment in the vapour up the column.

The columns were optimized for active area, weir height and downcomer clearance. It is important to have the maximum allowable active area as that is the contacting zone where mass transfer occurs. Downcomers are important in creating a vapour/liquid disengagement zone. Weir height should be optimized to maintain desired liquid level on the tray.

Based on the detailed design, using a standard tray spacing of 2ft, the height of the tray remained unchanged from DBM as number of trays remained the same. However, more detailed calculation of the column diameters was done. The diameter of the topping column, T-100 was 10.9ft compared to 10.5ft from hand calculation for DBM. This accounts for a 4% of error from the hand calculation. Thus, the design of T-100 can be deemed accurate since our DBM.

The diameter of the refining column, T-101 was 29.6ft compared to 30.2ft from hand calculation for DBM. This accounts for 2% of error from the hand calculation. The design of T-101 can also be deemed accurate since our DBM. This shows that the sample calculation for column sizing is still valid from the DBM. The equipment specification sheet for both the towers can be found in Appendix D.

The columns' temperature and composition profiles are as shown below in Figure 10 and Figure 11. The temperature and composition trend across each column remain unchanged after optimizations were done on our simulation since the DBM was completed.

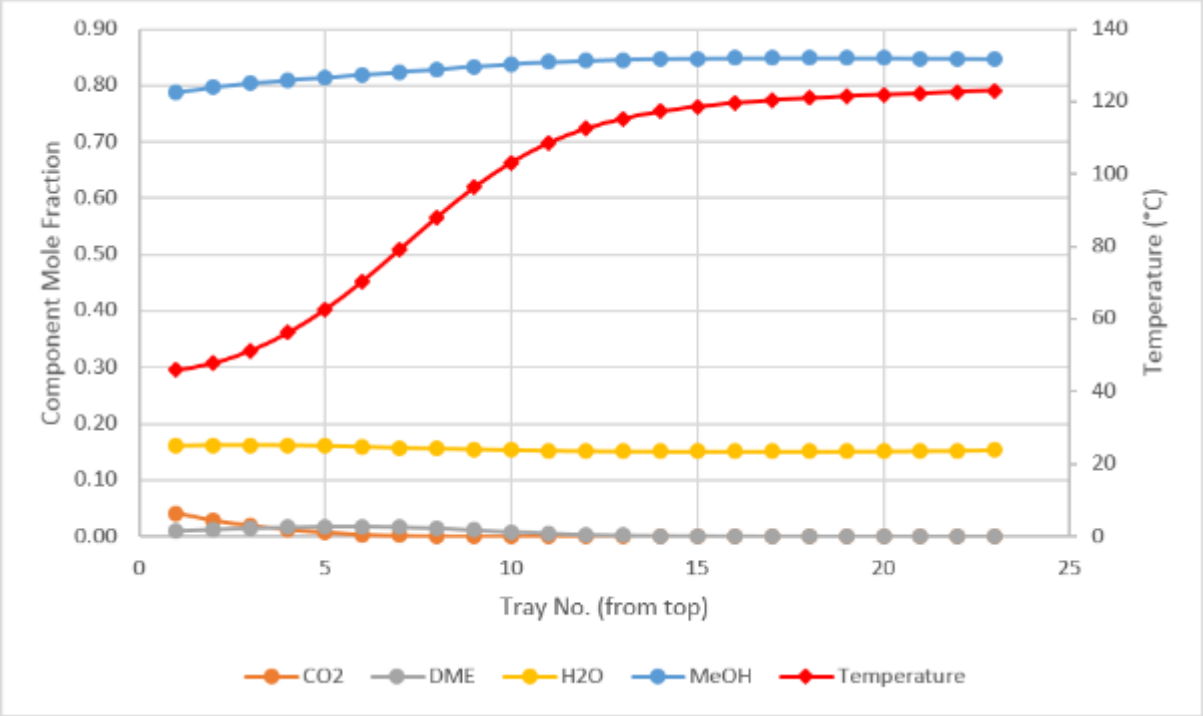

Figure 10: Topping column (T-100) temperature and composition profiles.

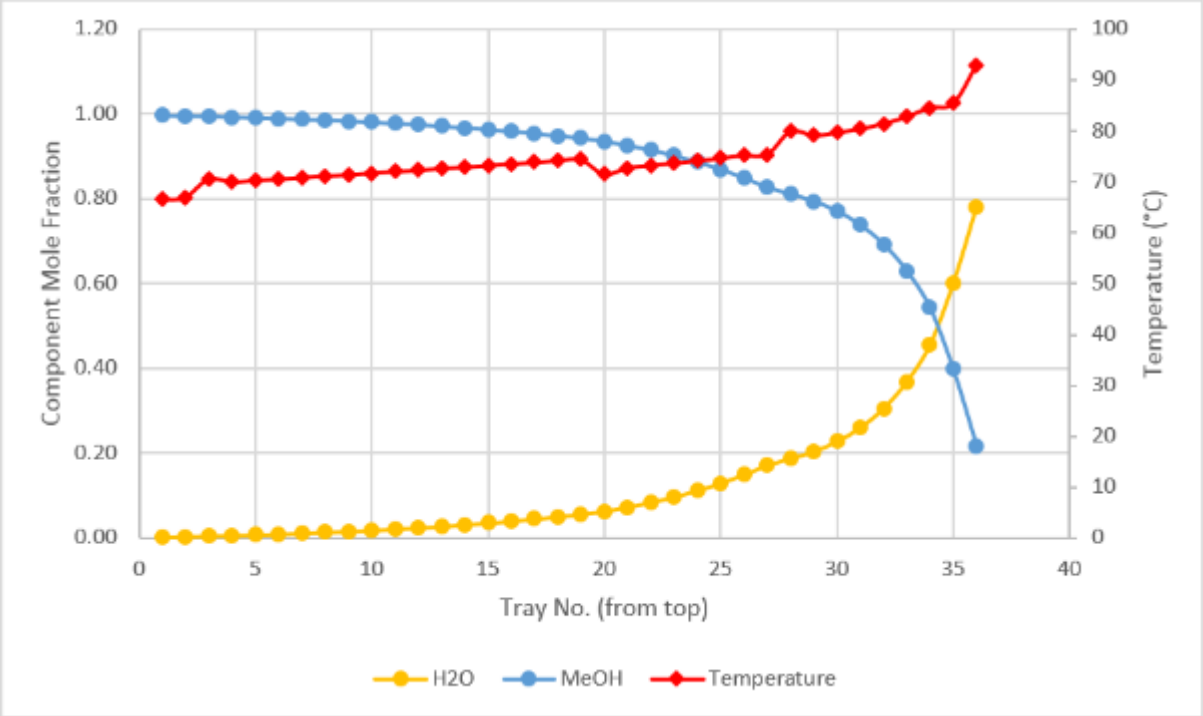

Figure 11: Refining column (T-101) temperature and composition profiles.

7.5 Separation Vessel Design

In our design, we have nine separation vessels used to separate vapour-liquid mixtures. These vessels are designed using Dr. Wayne Monnery's guide to design two-phase separators [54]. A vertical vessel is used when the vapour/liquid (V/L) ratio is high; otherwise a horizontal vessel is used. Vapour-liquid separators function using gravity separation where liquid falls to bottom of vessel by gravity. Vapour will travel up the vessel at a design velocity where entrainment of liquid droplets in the vapour is minimized.

Mist eliminators are used in our separation vessels to enhance removal of liquid droplets entrained in gas. Inlet diverters are also included in the design of our separation vessels as it ensures small amount of gas is carried with liquid. It also helps for efficient flow distribution of the two phases.

The design procedure for the vessels begins by determining the vapour/liquid ratio which consequently allows us to determine if it will be a vertical or horizontal separator. Once that is determined, vertical terminal vapour velocity, U_T is calculated and vapour velocity, U_V is set as $0.75U_T$. Next, vapour volumetric flow rate, Q_V is calculated which allows us to determine the vessel (inside) diameter, D_i or D_{VD}. As mentioned above, mist eliminator is used in our vessels and as such, 0.5 ft is added to the vessel diameter to accommodate a support ring [54]. Liquid volumetric flow rate, Q_L is also calculated which is then used to calculate holdup volume, V_H based on pre-determined holdup time, T_H. A surge time is also pre-determined and surge volume, V_S was obtained. From these calculated information, low liquid level height, H_{LLL}, normal liquid level, H_H, and surge height, H_S were found.

For vessels V-101A/B/C and V-104A/B, holdup time and surge time were based upon holdup time of 10 minutes and surge time of 3 minutes for interstage scrubber from the shortcut table provided. For V-100 and V-102, holdup time was determined as 5 minutes and surge time as 2 minutes. Whereas for V-103 and V-105, holdup time was 3 minutes and surge time was 2 minutes.

Since inlet diverter was included in our design, height from high liquid level to centerline of inlet nozzle, H_{LIN} was also determined. The disengagement height, H_D from the centerline of inlet nozzle to the vessel top tangent line was determined based on

equation given in 2-Phase Separator Sizing [54]. Since mist eliminator is used in the design, this contributes to another 1.5 ft as height for mist eliminator, H_{ME}. The total height, H_T of the vessel is finally determined by summing the calculated heights together.

The design procedure is similar for horizontal vessels as mentioned above with several other additional calculations. For horizontal vessels, thickness of shell and head, and surface area of the shell and heads can be determined from the design method by Dr. Monnery. This allows us to determine the vessel weight and by optimizing for minimum weight and keeping the range for L/D between 1.5 to 6.0, design for horizontal vessel is completed.

Sample calculation in designing the two-phase vessels, both vertical and horizontal, can be found in Appendix J. The length or height-to-diameter ratio for all vessels were optimized to be between the range of 1.5 to 6. The equipment specification sheet for all the separation vessels can be found in Appendix D.

7.6 Heat Exchanger, Reboiler, and Condenser Design

Heat exchangers are important units in the methanol plant design for heating and cooling process fluids. There are sixteen units modeled as heat exchangers for the whole process to provide the required temperature conditions and ensure the safe operations of the reaction system. For sizing purpose, the condensers and reboilers in distillation columns and compressors were done modeling as heat exchangers. The heat exchangers were sized using Aspen Exchanger Design and Rating tool, and all the units are modeled as shell and tube exchangers due to their extensive application in the petrochemical industry.

The sizing results for all the heat exchanger units has been summarized in the following table, and more detail can be found in their sizing specification sheets attached in Appendix D. The shell and tube heat exchangers for the process are sized under the desired operation conditions and specified to meet TEMA standards of construction. Based on different configurations of front end head, shell and rear end head, shell and tube exchangers are classified according to TEMA [55].

Table 3: Heat exchanger design summary.

Equipment	Duty (MW)	Type	Shell OD (in)	Tube Length (in)	Material
E-100A	-127	BKU	34.1	160	SS 316
E-101A	-73	BEP	57	263	SS 304
E-100B	-127	BKU	34.1	160	SS 316
E-101B	-73	BEP	57	263	SS 304
E-102A	-12	BEP	30	236	SS 304
E-102B	-13	BEP	41	230	SS 304
E-102C	-12	BEP	41	230	SS 304
E-103	-125	BEP	41	236	SS 304
E-104	-1	BEP	40	79	Carbon Steel
E-105	25	BKU	40	60	Carbon Steel
E-106A	-2	BEP	13	142	SS 304
E-106B	-1	BEP	15	224	SS 304
E-107	28	BEP	33	236	SS 304
E-108	-157	BEP	46	47.5	Carbon Steel
E-109	160	BKU	74	200	Carbon Steel
E-110	-6	BEP	20.1	189	SS 304

There are many factors that need to be considered when designing a heat exchanger, which includes service requirements, thermal duty, and material compatibility with process fluids. Among the service conditions, pressure drop is a major factor that need to be considered in the heat exchanger design. Since overall heat transfer coefficient can be optimized by maximizing shell side and tube side flow velocities, heat transfer is governed by allowable pressure drop as higher velocity means higher pressure drop. Hence, a proper pressure drop can help to optimize the heat exchanger performance. In the sizing processes, pressure drops of 35 kPa for cooling water and 70 kPa for other liquid streams are taken as a rule of thumb [56]. The pressure drops for gas and vapor streams are hard to predict, especially when phase change occurs. Therefore, the approximations based on system gauge pressure [56] were used and refined later to maintain a reasonable product flowrate.

Besides the technical requirements, another critical criterion for the exchangers is the ease of maintenance, which usually means cleaning or replacement of parts, tubing,

fittings, etc. damaged by ageing, vibration, corrosion throughout the service period [57]. Initially, most of the heat exchange units are modeled as BEM type due to its low cost and flexibility. A typical BEM design consists of front bonnet with an integral cover, straight tubes with a one pass shell and a fixed tubesheet bonnet. Since the tubesheet is welded to the shell and heads are bolts to the tube sheet, it's not feasible to clean the shell and tubes inside the fixed parts. Therefore, the exchangers have been revised to BEP design, which has an outside packed floating rear head with removable tube bundle. Like the BEM design, the BEP heat exchanger has a stationary front bonnet and one shell pass; however, one of the tubesheets is of the floating type. This design also allows for differential thermal expansion between the shell and tube bundle.

Other than exchanger type and pressure drop, fouling resistance also needs to be specified for more accurate equipment sizing. Fouling is defined as the formation and accumulation of unwanted materials deposit onto the processing equipment surfaces. These materials could form an insulation on the surface which can deteriorate the heat transfer performance of the surface [55]. On top of this, fouling increases the resistance to fluid flow, resulting in higher pressure drop across the heat exchanger. To effectively reflect the fouling factor in the heat transfer processes, TEMA Fouling Resistance values are used for the simulation [55]. Based on the maximum temperature and pressure of the equipment, stainless steel 304 and 316 were selected to construct the units. Since carbon steel was used in the distillation column design, it will be also used for their internal condensers and reboilers for consistency.

Due to different assumptions made during the calculation methods, there are huge variations between the calculated value and sizing result. What we found is that the calculated sizing specifications generally underestimate the optimum sizing requirement as a result of the theoretical conditions of the operations and material properties. Hand calculations to estimate heat exchanger size were presented in the DBM.

7.7 Piping Design

Capital investment on process piping is in the range of 25 – 40 % of the total plant investment and the power requirements for pumps and compressors, for which are

dependent on the line size, can be a considerable fraction of the total utility costs and GHG emissions.

As the diameter of a line increases, not only do the capital costs relating to material go up, but additional costs related to installation, fabrication, transportation, and so on also increase. In addition, not only are larger pipe sizes uncommon, but their material strength, related to the maximum allowable working pressure, decreases as well as. The positive however is that due to the decrease of fluid friction in larger pipes, the utilities for the continuous pumps and compressors decreases [58].

Turbulent fluid flow with a Reynolds number greater than 4000 was assumed within pipes to ensure proper mixing and uniformity. As such, initial optimal sizing of the piping was carried out using the following formulas from Sinnott (1999) and HYSYS process simulation data while following a rule of thumb that liquids are typically sized for velocities between 1 – 3 m/s, gas velocities are sized for velocities between 15 – 30 m/s and that pipe size are to be rounded up [58].

For Carbon Steel Pipes:

$$D_{Optimum} = 293G^{0.53}\rho^{-0.37} \text{ <mm>} \qquad \text{(Equation 2)}$$

For Stainless Steel and Alloy Pipes:

$$D_{Optimum} = 260G^{0.52}\rho^{-0.37} \text{ <mm>} \qquad \text{(Equation 3)}$$

Where:

G = Fluid mass flowrate $<\frac{kg}{s}>$

ρ = Fluid Density $<\frac{kg}{m^3}>$

Once optimal pipe sizing calculations has been calculated, multiple comparisons were then required to ensure the pipe size was available with material data of our selected piping material. ASME B31.3 Piping pressure rating tables for the specific material size and type was compared to simulation pressures and temperatures to ensure that the

Maximum Allowable Working Pressure (MAWP) would be suitable for that application, else adjustments were made in either line sizing or pipe material.

Lastly, pipe flanges according to ANSI B16.5 were selected for the MAWP of the pipelines to ensure the complete line was suitable for the process.

7.8 Compressor Design

Choice of type of compressor, whether it be axial, centrifugal, reciprocating, or rotary is dependent upon flow requirements, density of gas handled, in addition to the total head (compression ratio, for gases).

Axial compressors are able to handle a large flow volume and are typically more efficient than centrifugal compressors. Centrifugal compressors are, however, much more reliable and less prone to vulnerabilities, accommodate a wider range of operating conditions, and are more resistant to fouling. For these reasons, axial compressors are used for sweet natural gas, air, and non-corrosive gases.

Centrifugal compressors can operate continuously for extended periods of time. A reciprocating compressor would generally be used when required flow is too low for a centrifugal compressor, or the required head is too high that an unreasonably large number of stages would be necessary. For our process, all compressors were chosen to be centrifugal, as they provide the best reliability and performance characteristics.

Compressor specifications were determined by process simulation data from Aspen HYSYS, in conjunction with a commercial supplier of single and multi-stage compressors, Elliot Group ©.

7.9 Pump Design

Due to the amount and most utilized type of pump in the industry, they are divided into 2 main classes, Centrifugal and Others, such as Positive Displacement and Air Operated Diaphragm Pumps.

Centrifugal pumps are dominantly used as they are easily customizable to suit pumping applications, sold by many different vendors, incur less cost, generally have shorter delivery times, less maintenance, easily certified and readily available information.

By comparing the process conditions with the pump selection guide below, it was determined that centrifugal pumps would be able to handle our process requirements and was thus selected [58].

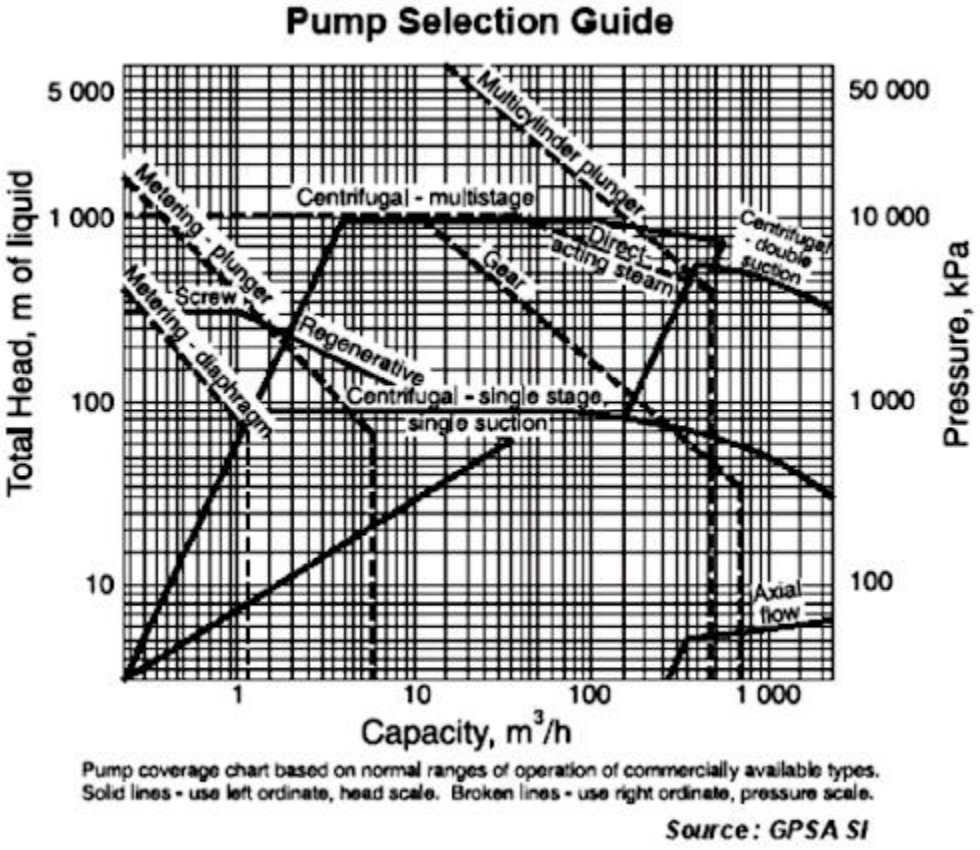

Figure 12: Pump selection guide from GPSA engineering handbook.

All pumps within our simulation were rated for continuous operation and any downtime would be costly for our overall operation. Thus, as shown in the P&ID, a parallel pumping system was implemented to ensure that a backup was always on standby and could easily be brought to service.

Additional pump design was completed with information incorporated from piping design, equipment and building layout as well as process controls required in the P&ID.

Mechanical Calculations:

The following Bernoulli equation, which is obtained from a mechanical energy balance on the system, was used to determine the head developed by the pump [58]:

$$\frac{-W_s}{g} = \frac{\Delta(v^2)}{2g} + \Delta z + \frac{\Delta P}{\rho g} + \frac{\Delta P_f}{\rho g} \qquad \text{(Equation 4)}$$

Where:

$-W_s/g$ = Total head <m>

$\Delta(v)$ = Change in fluid velocity <m/s>

g = Gravitational constant <m/s^2>

Δz = Change in elevation

ΔP = Pressure difference across the pump <Pa>

ρ = Fluid density <kg/m^3>

ΔP_f = Viscous Losses

This equation assumes the incompressibility of liquids.

Since there is no velocity change in the objects before and after the pump, $\Delta v = 0$ and therefore the equation now simplifies to:

$$\frac{-W_s}{g} = \Delta z + \frac{\Delta P}{\rho g} + \frac{\Delta P_f}{\rho g} \qquad \text{(Equation 5)}$$

The elevation difference (Δz) and pressure difference term across the pump (ΔP) is defined as the static head and pressure losses due to frictional forces (ΔP_f) is defined as the dynamic head. To calculate the dynamic head, the following equation and tables was used:

$$\Delta P_f = 8f\left(\frac{L_{eq}}{D}\right) \qquad \text{(Equation 6)}$$

Where:

f = Friction factor determined by the Moody Chart or Colebrook Equation

L_{eq} = Equivalent length of the pipe

D = Inner pipe diameter

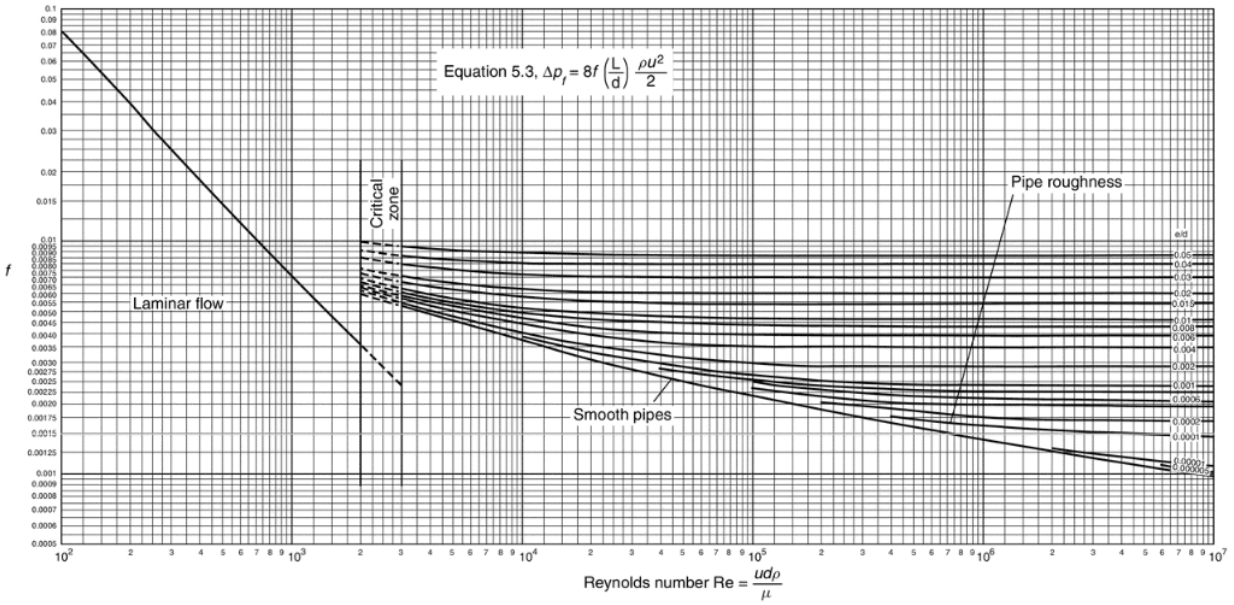

Figure 5.7. Pipe friction versus Reynolds number and relative roughness

Figure 13: Pipe friction versus Reynolds number and relative roughness.

Additionally, the Colebrook-White equation is mathematical method to calculate the friction factor in for turbulent fluids flow in pipes [59]. It can therefore be easily incorporated into excel worksheets. The equation is as follows:

$$\frac{1}{\sqrt{f}} = -2log_{10}(\frac{\varepsilon}{3.7D} + \frac{2.51}{R\sqrt{f}}) \qquad \text{(Equation 7)}$$

Where:

f = Darcy friction factor <Dimensionless>

ε = Absolute pipe roughness <in>

D = Inner pipe diameter

R = Reynolds number <Dimensionless>

Reynolds number was calculated using the following formula:

$$Re = \frac{\rho \times u \times d}{\mu} \qquad \text{(Equation 8)}$$

Where:

ρ = Fluid density <kg/m^3>

u = fluid velocity <m/s>

d = Inner diameter of pipe <m>

μ = fluid dynamic viscosity <kg/(m*s)>

Assumptions of absolute relative roughness for commercial steel and stainless steel pipes were assumed to be 0.046 and 0.015 mm respectively based on the following table:

Table 4: Pipe roughness.

Table 5.2. Pipe roughness

Material	Absolute roughness, mm
Drawn tubing	0.0015
Commercial steel pipe	0.046
Cast iron pipe	0.26
Concrete pipe	0.3 to 3.0

L_{eq} is calculated by the following formula:

$$L_{eq} = Length\ of\ pipe + (Total\ number\ of\ equivalent\ pipe\ diameters \times D) \qquad \text{(Equation 9)}$$

Where:

D = Inner pipe diameter

Total number of equivalent pipe diameters is determined from identifying all valves and fittings from the P&ID, estimating the elbows required based on the site and equipment layout, and referencing the following table:

Table 5: Pressure loss in pipe fittings and valves (for turbulent flow).

Table 5.3. Pressure loss in pipe fittings and valves (for turbulent flow)

Fitting or valve	K, number of velocity heads	number of equivalent pipe diameters
45° standard elbow	0.35	15
45° long radius elbow	0.2	10
90° standard radius elbow	0.6–0.8	30–40
90° standard long elbow	0.45	23
90° square elbow	1.5	75
Tee-entry from leg	1.2	60
Tee-entry into leg	1.8	90
Union and coupling	0.04	2
Sharp reduction (tank outlet)	0.5	25
Sudden expansion (tank inlet)	1.0	50
Gate valve		
fully open	0.15	7.5
1/4 open	16	800
1/2 open	4	200
3/4 open	1	40
Globe valve, bevel seat-		
fully open	6	300
1/2 open	8.5	450
Plug valve - open	0.4	18

Lastly, the power in Watts expected to be required by the pump is calculated by the following:

$$Power = -W_s \times \frac{G}{n} \qquad \text{(Equation 10)}$$

Where:

-Ws = Shaft work done by the pump, obtained from the first Bernoulli Equation <J/kg>

G = Mass flow rate of the liquid <kg/s>

n = Pump efficiency

Lastly, the Net Positive Suction Head available (NPSHa) for the pump to ensure protection from cavitation is calculated from the following formula:

$$NPSHa = \frac{P}{\rho g} + H - \frac{\Delta P_f}{\rho g} - \frac{P_v}{\rho g} \qquad \text{(Equation 11)}$$

Where:

P = Pressure above the liquid in the feed vessel <Pa>

H = Minimum height of liquid above the pump section <m>

ΔP_f = Viscous pressure losses in the suction piping <Pa>

Pv = Vapour pressure of the liquid at the pump section <Pa>

ρ = Fluid density <kg/m^3>

g = Gravitational constant <m/s^2>

As this calculation requires a liquid height from the pump to lowest level in the feed tank and piping layout from the feed tank to the pumps, it has to be finalized after accurate equipment and piping orientation / layout has been completed (i.e to scale site 3D modeling and isometric drawings). Preliminary calculation can be done to give the pump vendor an estimated NPSHa for which he can find suitable pumps for, else the pump vendor can state a minimum NSPHa required, for which may be accommodated by design changes.

8.0 Economics

Bare module cost is defined as the sum of the direct and indirect expenses for purchasing and installing equipment. To estimate the bare module cost and purchase cost of equipment, the following relations proposed by Turton et al. [60] were used:

$$C_{BM} = C_P^\circ * F_{BM} = C_P^\circ (B_1 + B_2 F_M F_P) \qquad \text{(Equation 12)}$$

$$\log C_P^\circ = K_1 + K_2 \log(S) + K_3 [\log(S)]^2 \qquad \text{(Equation 13)}$$

Where S denotes a parameter for equipment size. B_1 and B_2 are constants.

K_1, K_2, and K_3 are equipment specific constants.

C_P° is the purchase cost.

F_{BM} is the bare module cost factor.

C_{BM} is the bare module equipment cost.

F_P is the pressure factor.

Values for constants were obtained from data tables developed by Turton et al. [60] and are specific to each process unit and material chosen. A current Chemical Engineering Plant Cost Index (CEPCI) of 620 was used. The CEPCI consists of a composite index composed of four separate sub-indexes that include equipment, construction labor, buildings, and engineering & supervision. The CEPCI is an index to adjust plant construction costs from one time period to another. The following is an order of magnitude estimate, utilizing capacity factored and parametric estimates to determine equipment costs.

Table 6: Bare module cost for major equipment.

Name	Equipment	Material	Bare Module Cost ($)
Distillation Tower Topping Column	T-100	Carbon Steel	684 000
Topping Column Condenser	E-104	Carbon Steel	133 300
Topping Column Reboiler	E-105	Carbon Steel	136 700
Distillation Tower Refining Column	T-101	Carbon Steel	11 810 000
Refining Column Condenser	E-108	Carbon Steel	541 300
Refining Column Reboiler	E-109	Carbon Steel	488 700
Waste Heat Boiler	E-100A	Stainless Steel	4 095 700
Cold Water Cooler	E-100B	Stainless Steel	885 300
Compressed Feed Gas Fan Cooler	E-101A	Carbon Steel	115 100
Product Liquid-Gas Separator	V-103	Carbon Steel	2 780 000
Water Knockout Drum	V-100	Stainless Steel	1 780 000
Startup Heater/Steam Generating Reactor	R-100	Chromium Molybdenum	689 760
Gas-Gas Exchange Reactor	R-101	Chromium Molybdenum	4 017 600
Dry Feed Gas Compressor	K-100	Carbon Steel	39 600 000
Recycle Compressor	K-103	Carbon Steel	6 770 000
Main Recycle Compressor	K-102	Carbon Steel	2 765 000
Lean Syngas Compressor	K-101	Carbon Steel	1 145 000
Cold Water Cooler	E-110	Stainless Steel	267 700
Start-up Steam Heater	E-107	Carbon Steel	1 121 100
PSA Unit	C-100	Stainless Steel	24 762 986
		Total	**104 589 246**

Table 7: Classification of capital cost estimates [61].

Classification of Capital Cost Estimates – AACE International Recommended Cost Estimation Classification System				
Class/Type	**Purpose**	**Methodology**	**Accuracy**	**Level of Project Completion**
Class 5: Order of Magnitude Estimates	Initial feasibility study or screening	Capacity Factored, Parametric Models, Judgment, or Analogy	L: -20% to -50% H: +30% to +100%	0-2%
Class 4: Study or Preliminary Estimates	Concept study or feasibility	Equipment Factored or Parametric Models	L: -15% to -30% H: +20% to +50%	1-15%
Class 3: Definitive Estimates	Budget authorization or control	Semi-Detailed Unit Costs with Assembly Level Line Items	L: -10% to -20% H: +10% to +30%	10-40%
Class 2: Detailed Estimates	Control or bid/tender	Detailed Unit Cost with Forced Detailed Take-Off	L: -5% to -15% H: +5% to +20%	30-70%
Class 1: Check Estimates	Check estimate or bid/tender	Detailed Unit Cost with Detailed Takeoff	L: -3% to -10% H: +3% to +15%	50-100%

Cost data exhibit scatter due to varying qualities of equipment design/manufacturing, fabrication methods, market conditions, vendor profit etc. As a result, published equipment cost data can easily be ±25%.

8.1 Economic Summary

To gain a sense of what similar plants have costed in the past, and to make an order of magnitude estimate of plant cost, a known cost of a prior similar plant will be scaled up.

The capital cost of a plant can be related to capacity by the equation:

$$C_2 = aS_2^n \qquad \text{(Equation 14)}$$

Where S denotes capacity.

For the Methanol via Steam Reforming and Synthesis process developed by Davy Process Tech, a = 2.775, and n = 0.6. This gives an approximate estimate of ~$460MM. A similar methanol synthesis plant, developed by Methanex Corporation in Geismar, LA cost ~$550MM. The total plant cost can be estimated by a factored estimate. In this method the bare module cost is determined for each piece of equipment and then a multiplication factor is applied to ascertain an estimate. The multiplication factors used in table 12 are typical to that of a fluid processing plant in industry. Captured hydrogen byproduct will be sold to help alleviate materials, labor, and utility costs.

Table 8: Product value.

Name of Material	Price ($/ton)	Annual Amount (tons/year)	Annual Value of Product ($MM)
Methanol	342	1 825 000	624.15

Table 9: Raw materials value.

Name of Material	Price ($/kg)	Annual Amount (tons/year)	Annual Raw Materials Cost ($MM)
Syngas	0.025	4 434 750	110.85

Table 10: Annual operating labor costs.

Number of Operators per Shift	Shifts per Day	Operator Rate ($/h)	Annual Operating Labour Cost ($MM/y)
3	3	33.67	0.808

The plant will operate continuously, with a plant availability of 91.3%, and operate for 8000 hours/year.

Table 11: Utility costs.

Utility	**Unit Cost ($)**	**Cost Units**
Process Air	0.45	$/m^3
Instrument Air	0.90	$/m^3
Purchased Electricity	0.068	$/kWh
Saturated Steam 3550 kPa	8.00	$/1000kg
Saturated Steam 790 kPa	6.00	$/1000kg
Waste Water Disposal	0.53	$/m^3
Waste Water Treatment	0.53	$/m^3
Waste Disposal (Hazardous)	145.00	$/1000kg
Waste Disposal (Non-Hazardous)	36.00	$/1000kg
Water - Cooling	0.08	$/m^3
Water – Process (General)	0.53	$/m^3
Water – Process (Distilled)	0.90	$/m^3

Table 12: Estimation of capital investment based on delivered equipment cost.

Direct Costs		Fraction of delivered equipment	Calculated Values ($MM)
	Purchased equipment delivered		104.89
	Instrumentation and controls (installed)	0.36	37.65
	Piping (installed)	0.68	71.11
	Electrical Systems (installed)	0.11	11.50
	Buildings (including services)	0.18	18.82
	Yard improvements	0.10	10.46
	Service facilities (installed)	0.70	73.21
	Total direct plant cost		**327.64**
Indirect Costs	Engineering and supervision	0.33	34.61
	Construction expenses	0.41	42.88
	Legal expenses	0.04	4.18
	Contractors fee	0.22	23.0
	Contingency	0.44	46.02
	Total indirect plant cost		**150.69**
Fixed Capital Investment			**478.33**
Working Capital		0.89	**93.35**
Total Capital Investment			**571.68**

This figure of $572MM is quite reasonable and is in line with what similar plants have costed in the past. Typically, main process equipment is responsible for 20-40% of fixed capital investment in a chemical engineering plant [62].

Table 13: Economic evaluation.

Year Ending at Time	-2	-1	0	1	2	3	4	5	6	7	8	9	10
Fixed Capital ($MM)	-71.75	-170.76	-248.83										
Working Capital ($MM)			-95.89										
Total Capital Investment ($MM)	-71.75	-170.76	-344.72										
Startup Cost ($MM)				-49.13									
Operating Rate, Fraction of Capacity				0.50	0.90	1	1	1	1	1	1	1	1
Annual Sales ($MM)				312.08	561.74	624.15	624.15	624.15	624.15	624.15	624.15	624.15	624.15
Annual Total Product Cost ($MM)				-140.98	-208.75	-229.48	-234.07	-238.76	-243.53	-248.40	-253.37	-258.44	-263.61
Annual Gross Profit ($MM)				23.69	195.76	300.33	333.47	328.79	352.32	375.75	370.78	365.71	360.54
Annual Net Profit ($MM)				15.40	127.24	195.21	216.76	213.71	229.01	244.24	241.01	237.71	234.35
Annual Operating Cash Flow ($MM)				113.67	284.47	289.55	273.36	270.32	257.31	244.24	241.01	237.71	234.35
Total Annual Cash Flow ($MM)	-71.75	-170.76	-344.72	113.67	284.47	289.55	273.36	270.32	257.31	244.24	241.01	237.71	234.35

Startup cost was assumed to be 10% of fixed capital investment.

Table 14: Profitability measures.

Return on investment, ROI, ave. %/y	**33.3**	
Payback period, y	**2.0**	
Net return ($MM)	**107.38**	at m_{ar} = 15.0 %/y

m_{ar} denotes minimum acceptable rate of return.

Table 15: Profitability measures including time value of money, with annual end-of-year cash flows and discounting.

Year Ending at Time	-2	-1	0	1	2	3	4	5	6	7	8	9	10	Row Sum
Present Worth Factor	1.32	1.15	1.00	0.87	0.76	0.66	0.57	0.50	0.43	0.38	0.33	0.28	0.25	
Present Worth of Annual Cash Flows ($MM)	-94.89	-196.38	-344.72	98.84	215.10	190.38	156.29	134.40	111.24	91.82	78.79	67.57	57.93	566.38

Net Present Worth = $566.38MM at discount rate of 15%/y.

Discounted Cash Flow Rate of Return, DCFRR = 15.2%/y.

Table 16: Profitability measures including time value of money, with continuous cash flows and discounting.

Year Ending at Time	-2	-1	0	1	2	3	4	5	6	7	8	9	10	Row Sum
Present Worth Factor	1.42	1.23	1.07	0.93	0.81	0.71	0.61	0.53	0.46	0.40	0.35	0.31	0.27	
Present Worth of Annual Cash Flows ($MM)	-101.84	-210.76	-369.97	106.08	230.86	204.33	167.74	144.24	119.39	98.54	84.56	72.52	62.17	607.87

Net Present Worth = $607.87MM at discount rate of 14%/y.

Discounted Cash Flow Rate of Return, DCFRR = 14.1%/y.

For the above analysis, an income tax rate of 35% was used. Construction and product cost inflation was assumed to be 2%.

8.2 Sensitivity Analysis

There are a number of risks associated with a methanol plant, and the plant is sensitive to a variety of factors. The viability of the methanol plant is dependent on the cost of raw feed material, and the pricing of methanol itself. However, as can be seen from the figure below, the price has generally trended upwards over the past. Price of raw feed, syngas, is presumably dependent on natural gas, and tends to be cyclical, and is currently at historic lows [63].

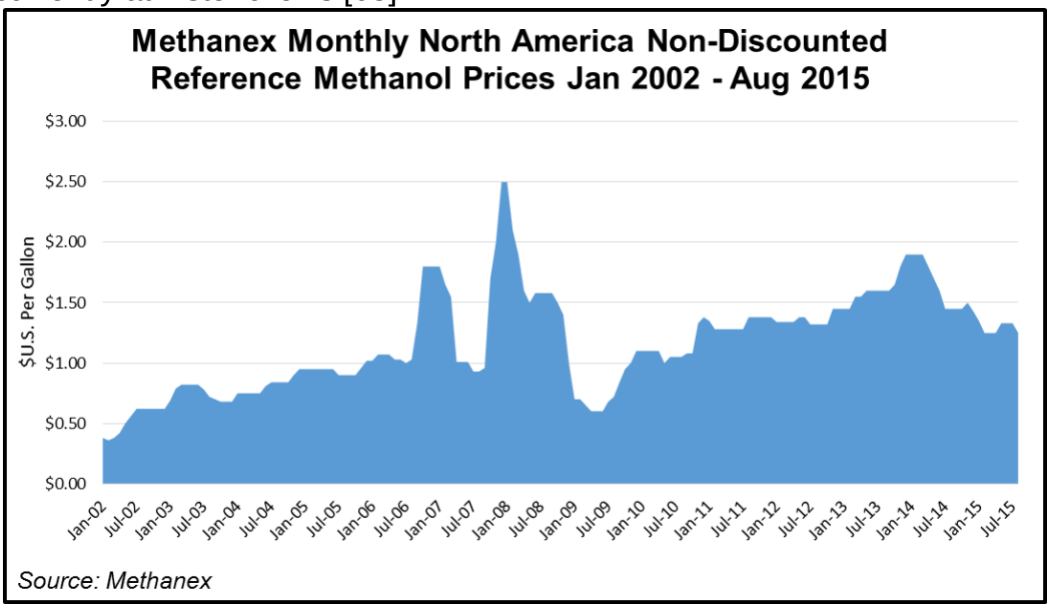

Figure 14: Methanex monthly North America non-discounted reference methanol prices (January 2002-August 2015) [63].

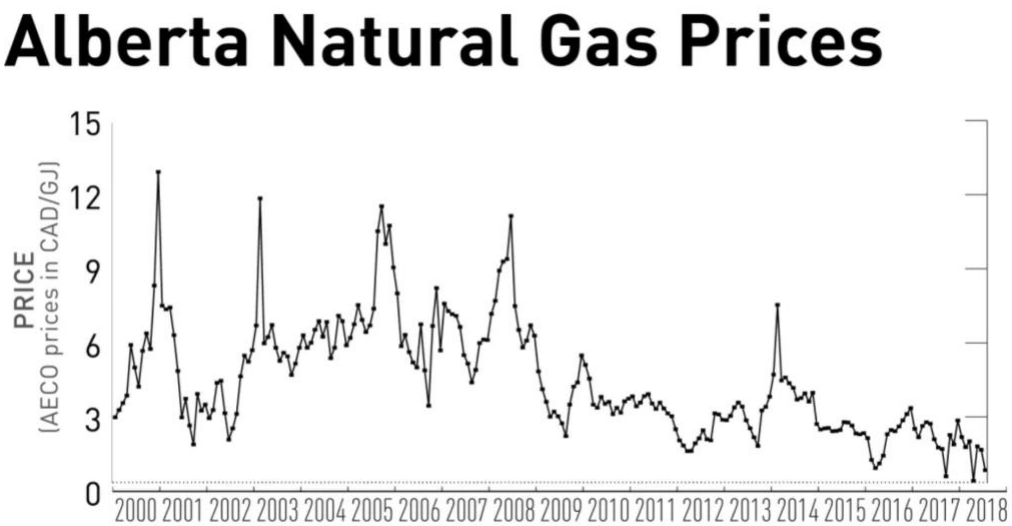

Figure 15: Alberta natural gas prices (2000-2018) [64].

Another potential risk factor is technology risk. Methanol production at large scales is technologically mature. However, many companies are pursuing the development of small-scale plants that may pose risks as unknown or unanticipated technologies are scaled up.

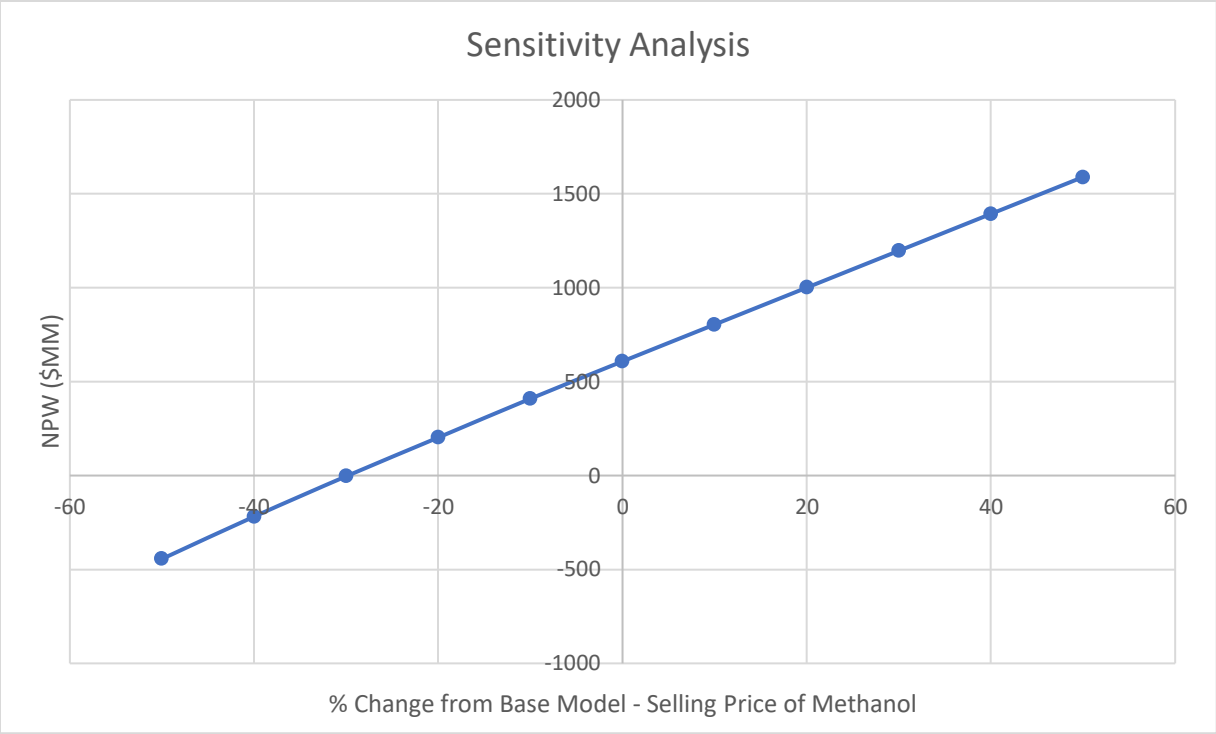

Figure 16: Sensitivity analysis on changes in selling price of methanol on NPW (with continuous cash flows and discounting).

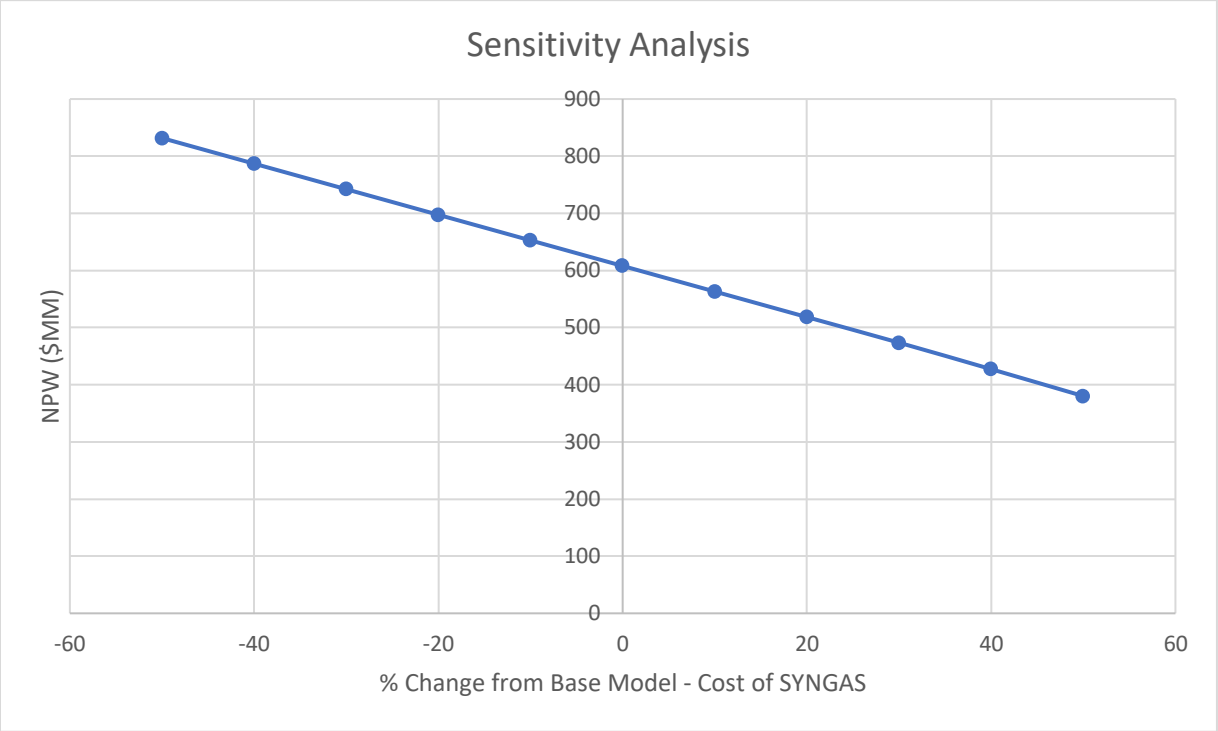

Figure 17: Sensitivity analysis on changes in cost of syngas on NPW (with continuous cash flows and discounting).

The following two figures illustrate the relationship between changes in price of methanol, and in the cost of syngas and their corresponding effects on NPW, with continuous cash flows and discounting. It is evident that our process is quite economically sensitive to fluctuations in the selling price of methanol, and less so to cost of syngas feed.

9.0 Process Safety and Environmental Impacts

9.1 Process Safety

In an engineering design, it is extremely important to consider safety of the design and reduce or mitigate any risks identified. Inadequate hazard identification and risk assessment can cause loss of lives, loss of profit and negative public opinion of the company.

Material hazards such as toxicity of our feed and products and susceptibility to fire and ignition were discussed in our Design Basis Memorandum (DBM) as attached in Appendix L. Hazard and operability (HAZOP) analysis on major equipment were also completed and included in our DBM. In this report, we will be discussing process hazards due to equipment operation and our proposed mitigation techniques. HAZOP analysis for our Pressure-Swing Adsorption (PSA) unit that was black boxed in DBM is also included.

One of the most serious hazards in a chemical plant operation is overpressure. This happens when there is mass or energy accumulation in a contained volume. As process controls may not be able to respond to this situation quick enough, we have included pressure relief valves (PRV). Pressure relief valves can avoid vessel rupture or explosion that could endanger lives due to pressure rise.

High temperature over which the equipment was designed for can cause structural failure and initiate disaster. Very low temperatures can cause embrittlement and stress cracking in metals leading to structural failure too. Thus, it is very important to have temperature controls in place. These are included in our P&ID not just for optimization of our design but also for safety reasons.

Fires in chemical plants can lead to damage of equipment and control systems, causing further hazards such as overpressure and explosion. In our design, flare stacks are included. If not positioned correctly, they can contribute to fire in the plant. Thus, in our design as can be seen on our site layout and plot plan in Appendix H and I, the flare stacks are positioned upwind and away from the plant.

Critical alarms are also included in our plant design. This is a part of our active engineering risk control strategy. Alarms would interrupt the chain of event following

initiation and alert operators. Followed by control strategies in place, this increases level of confidence in our design safety. High-level and low-level alarms are installed for all our vessels and can be referred to in our P&ID in Appendix C.

Hazard and operability study (HAZOP) is a qualitative technique of risk evaluation. As mentioned, we have performed HAZOP analysis for major equipment in our design that are included in our DBM. We have also performed HAZOP study for our Pressure-Swing Adsorption unit and it can be found in Appendix F.

9.2 Environmental Impacts

The production of methanol from natural gas using steam reforming is a relatively clean and environmentally safe process. Typical commercial processes produce about 600 to 1200 pounds of carbon dioxide per ton of methanol produced [65]. Therefore, while the methanol produced may be relatively non-polluting compared to gasoline and diesel fuel when it is combusted, the manufacturing process of methanol may in fact be a substantial source of greenhouse gases.

In our process, large amount of water and steam are used for heating and cooling processes, and therefore quite clean except for traces of solids and a little dissolved gas. The system has unreacted synthesis gases, which originally includes up to 15% carbon dioxide. Also, two purge streams are removed to prevent the build up of inert gases in the system. The remainder of the streams are recycled to the reaction system. In this way, carbon dioxide, as well as carbon monoxide and methane, may be recycled through the system essentially to extinction except for the purge streams. The impact of purge stream emissions is elaborated in the following Greenhouse Gases (GHG) calculation section.

Besides the gas effluents, the process also generates liquid waste to the environment. The product stream of topping distillation column mainly consists of methanol and water, while higher alcohols with methanol and water yield from refining column. Large amount of methanol and higher alcohols need to be prevented from mixing with groundwater to avoid contamination of drinking water, but these liquid effluents can be treated with biological method to break down the polluters [66].

Overall, the environmental impact of the methanol production is relatively small compared to other chemical and petrochemical process. The process complies with regulations such as Clean Air Act and Clean Water Act as most of the effluents can be properly treated and discharged to minimize the impact to the environment. Therefore, it is considered a clean and environmentally safe process.

9.3 Greenhouse Gas Calculations

Global warming from the increase in greenhouse gases emission has become a major scientific and political issue during the past decade. As concerns over GHG emission been recognized worldwide, attention being focus on the chemical production process, including methanol manufacture. Having synthesis gas as feedstock, our process definitely has the potential to impact the environment. Synthesis gas, which is the feed to our process, is mainly composed of hydrogen, carbon monoxide, and also carbon dioxide and methane. The latter two components are leading cause of greenhouse effect.

Even though fugitive and accidental emissions also could happen, we mainly focus on the waste streams during normal operation conditions [67]. GHG emissions associated with our project basically have two forms: One is our direct flared gas before entering the recycle stream for adjusting the reaction stoichiometric ratio, and the other one is due to the plant electricity consumption. Based on our simulation results, the GHG emission has been calculated and shown in the Table 17. Although CO, H_2, N_2 also contributes to global warming and other environmental issues, our main focus is on the CO_2 and CH_4 emissions as they are direct causes to greenhouse effect. An equivalent CO_2 emission of 0.58 tons per metric ton methanol produced is reported as the plant gas emission to the atmosphere. Compared to Ammonia and other chemical and petrochemical production, our CO_2 emission is on the relatively low side of general chemical manufacturing process.

Table 17: Component total emission and equivalent CO_2 emission.

Components	Total Emission (kg/h)	GWP	Equivalent CO_2 Emission(kg/h)
CO_2	14266.5	1	14266.5

Methane	2990.4	25	74760.5
CO	327.0	-	-
H_2	2628.5	-	-
Nitrogen	425.5	-	-
Electricity	48952(kW)	-	34600
Total	-	-	123627

10.0 Conclusions and Recommendations

As expected for the final deliverable of the project, detailed design of all equipment was performed and specification sheets for every piece of equipment are included. All equipment shows less than 10% error from sizing done in Design Basis Memorandum (DBM). This shows the assumptions made for hand calculations in DBM shows reliable results. Our process selection remains the same as Lurgi Megamethanol process, however we have revised our site location. Our project has been relocated to US Gulf Coast (USGC) from the initial suggested location of Grand Prairie, Alberta due to economic and logistics benefits.

Although our process remains the same, some optimization was done. This includes the production of Medium Pressure Steam (MPS) over Low Pressure Steam (LPS) in our Steam Raising Reactor, R-100. This change since DBM happened as we revised our design and realized internal mass transfer limitations were not considered initially. We have also decided to send H_2 lean syngas stream to be compressed by K-101 and then through K-103A/B in order to prevent the addition of another multi-stage compressor in our design.

Detailed design of all equipment including the Pressure Swing Adsorption (PSA) unit was completed. The design is of a four bed PSA system based on Linde's hydrogen recovery technology with Zeolite 5A and Activated Carbon adsorbents. As this design is based on conservative hand calculations, we believe dynamic simulation using Aspen Adsorption would allow us to make comparison on the accuracy of our design. Due to constraints beyond our control, we have decided that our hand calculations for PSA detailed design are sufficient for the scope of this project.

Economic analysis for our process yielded a total capital investment of approximately $572MM, with fixed capital investment of $478.33MM of which $327.64MM were direct expenses, and $150.69MM were indirect expenses. Using annual end of year cash flows, net present worth (NPW) was determined to be $566.38MM and discounted cash flow rate of return (DCFRR) was 15.2%. Continuous cash flow analysis yielded an NPW of $607.87MM and DCFRR of 14.1%. In either analysis, expected return on investment (ROI) was 33.3% and payback period was

only 2.0 years. The current selling price of methanol is $342/ton, and this was used in the analysis. Syngas price used is $25/TCM (thousand cubic meters). Sensitivity analysis has been completed and addressed in our DBM.

It is extremely important that our design is safe and up to environmental regulatory standards. We have incorporated safety aspects through control strategies and alarms. However, more detailed safety analysis is definitely required to be performed on top of our preliminary Hazard and Operability (HAZOP) analyses. To quantify our project's environmental impact, we have performed a Greenhouse Gas (GHG) calculation. An equivalent CO_2 emission of 124 000 kg/h is calculated for our plant. More detailed Life Cycle Analysis (LCA) and GHG calculation can also be performed but was outside the scope of our work.

Based on the economic benefits and the success of our detailed design, our team whole-heartedly agrees that this project is worth pursuing.

References

[1] 2019, February 25. Methanol Market Share, Size, Demand, Price & Trends, Application, Opportunities, Sales & Revenue, Industry Growth, Key Players and Global Forecast to 2023. Retrieved from https://www.reuters.com/brandfeatures/venture- capital/article?id=85404.

[2] Mouljin et al. Chemical Process Technology (2nd Ed.).

[3] Sheldon, D. Methanol Production – A Technical History. (Johnson Matthey Technology Review)

[4] Mansfield, K. Nitrogen, 1996, 221, 27 (Johnson Matthey Technology Review)

[5] Lurgi MegaMethanol™. (2018, July 12). Retrieved from https://www.engineering-airliquide.com/lurgi-megamethanol.

[6] Cheng. Methanol Production and Use. Pg 111.

[7] Bozzano, G.,& Manenti, F. (2016). Efficient methanol synthesis: Perspectives, technologies and optimization strategies. Progress in Energy and Combustion Science, 56(2016), 71-105.

[8] Meyers, R. A. (2005). *Handbook of petrochemicals production processes*. New York: McGraw-Hill.

[9] Speight, J. G. (2019). Handbook of petrochemical processes: Part 7. Boca Raton, FL: CRC Press, Taylor & Francis Group.

[10] Sheldon, D. (2017) Methanol Production - A Technical History. Johnson Matthey Technological Review, 61(3), 172-182.

[11] Blumberg, T., Morosuk, T.,& Tsatsaronis, G. (2017). A Comparative Exergoeconomic Evaluation of the Synthesis Routes for Methanol Production from Natural Gas. Applied Sciences, 7(12), 1213.

[12] Al-Fadli, A., Soliman, M.,& Froment G. (1994) Steady State Simulation of a Multi-Bed Adiabatic Reactor for Methanol Production. Engineering Science, 7(Special Issue), 101- 133.

[13] Leonzio, G., Zondervan, E.,& Foscolo, P. (2018) Methanol Production by CO2 hydrogenation: Analysis and simulation of reactor performance. International Journal of Hydrogen Energy, 44(2019), 7915-7933.

[14] Wu, Y.,& Gidaspow, D. (1997) Hydrodynamic simulation of methanol synthesis in gas-liquid slurry bubble column reactors. Chemical Engineering Science, 55(2000), 573- 587.

[15] Methanex (n.d.). Retrieved from https://www.methanex.com/sites/default/files/investor/MEOH%20Presentation%20-%20May.pdf

[16] Mittasch, A., Pier, M. BASF AG, 'Ausführung Organischer Katalysen', German Patent 415,686; 1925.

[17] Yim, J. (2011). Asia Olefin Market Outlook. Asia Petrochemical Industry Conference, Fukoka, Japan.

[18] 2019, February 25. Methanol Market Share, Size, Demand, Price & Trends, Application, Opportunities, Sales & Revenue, Industry Growth, Key Players and Global Forecast to 2023. Retrieved from https://www.reuters.com/brandfeatures/venture- capital/article?id=85404.

[19] Montney. (n.d.). Retrieved from https://www.aer.ca/providing-information/data-and-reports/statistical-reports/st98/reserves/low-permeability-and-shale-area-assessment/montney

[20] U.S. Department of Energy. (2018, December). U.S. Crude Oil and Natural Gas Proved Reserves, Year-End 2018. Retrieved from https://www.eia.gov/naturalgas/crudeoilreserves/pdf/usreserves.pdf

[21] Canadian Energy Research Institute. (2016, October). Study 160: Competitive Analysis of the Canadian Petrochemical Sector. Retrieved from https://www.nrcan.gc.ca/sites/www.nrcan.gc.ca/files/energy/pdf/GenEnergy/CERI%20-%20Competitive%20Analys%20of%20the%20Canadian%20Petrochemical%20Sector.pdf

[22] The Global Syngas Technologies Council. (n.d.). Retrieved from https://www.globalsyngas.org/resources/map-of-gasification-facilities/

[23] Canadian Energy Research Institute. (2018, March). Economic Impacts and Market Challenges for the Methane to Derivatives Petrochemical Sub-Sector. Retrieved from https://ceri.ca/assets/files/Study_169_Full_Report.pdf

[24] Canadian Energy Research Institute. (2015, August). Examining the Expansion Potential of the Petrochemical Industry in Canada. Retrieved from https://ceri.ca/assets/files/Study_153_Full_Report.pdf

[25] (2019, April 22). Oil and Gas Prices. Retrieved from https://www.oilsandsmagazine.com/energy-statistics/oil-and-gas-prices

[26] Paraskova, T. (2019, March 21). Canada's Natural Gas Crisis Is Going Under The Radar. Retrieved from https://oilprice.com/Energy/Gas-Prices/Canadas-Natural-Gas-Crisis-Is-Going-Under-The-Radar.html

[27] Banquy, W. L. US Patent No. 4,888,130. (1989).

[28] Foley, M. Chemical Engineering Department, University of Calgary, Calgary, AB, Canada. Personal communication, November 2018.

[29] Dalena, F., Senatore, A., Basile, M., Knani, S., Basile, A., & Iulianelli, A. (2018). Advances in Methanol Production and Utilization, with Particular Emphasis toward Hydrogen Generation via Membrane Reactor Technology. Membranes, 8(4), 98. doi: 10.3390/membranes8040098

[30] Linde Engineering. (n.d.). Hydrogen Recovery by Pressure Swing Adsorption. Retrieved from https://www.linde-engineering.com/en/images/HA_H_1_1_e_09_150dpi_NB_tcm19-6130.pdf

[31] Fong et al. US Patent No. 5,496,859. (1996).

[32] Twigg, M. V., & Spencer, M. S. (n.d.). Deactivation of Copper Metal Catalysts for Methanol Decomposition, Methanol Steam Reforming and Methanol Synthesis. Retrieved from https://link.springer.com/article/10.1023/A:1023567718303.

[33] Jahan, A., Mustapha, F., Sapuan, S. M., Ismail, M. Y., & Bahraminasab, M. (2011). A framework for weighting of criteria in ranking stage of material selection process. The International Journal of Advanced Manufacturing Technology, 58(1-4), 411–420. doi: 10.1007/s00170-011-3366-7

[34] Chemical Publishing Company Inc. (n.d.). Practical Boiler Water Treatment Handbook. S.l.

[35] Mackey, E. D., & Seacord, T. F. (2017). Guidelines for Using Stainless Steel in the Water and Desalination Industries. Journal - American Water Works Association, 109. doi: 10.5942/jawwa.2017.109.0044

[36] Marchi, C. W. S., & Somerday, B. P. (2012). Technical reference for hydrogen compatibility of materials. doi: 10.2172/1055634

[37] Compatibility of Metals & Alloys in Neat Methanol Service. (n.d.). Retrieved from http://www.methanol.org/wp-content/uploads/2016/06/Compatibility-of-Metals-Alloys-in-Neat-Methanol-Service.pdf.

[38] Park, N., Park, M.-J., Lee, Y.-J., Ha, K.-S., & Jun, K.-W. (2014). Kinetic modeling of methanol synthesis over commercial catalysts based on three-site adsorption. *Fuel Processing Technology*, *125*, 139–147. doi: 10.1016/j.fuproc.2014.03.041

[39] Flessner, U. (2015). Clariant Catalysts: Industrial Methanol Catalysts – Today and Tomorrow. Retrieved from https://eu-ems.com/event_images/presentations/Uwe%20Flessner.pdf

[40] Haldor Topsoe, K., Aaseberg-Petersen, C. S. Nielsen, I. Dybkjaer, J. Perregaard. (n.d.). Large Scale Methanol Production from Natural Gas.

[41] Ng, K., et. al. (1999). Kinetics and modelling of dimethyl ether synthesis from synthesis gas. *Chem. Eng. Sci.*

[42] Graaf, G., et. al. (1988). Kinetics of Low-Pressure Methanol Synthesis. *Chem. Eng. Sci.*

[43] Clariant Ltd. (2018, August 12). MegaMax® 800. Retrieved from https://www.clariant.com/en/Solutions/Products/2018/02/14/13/39/MegaMax-800

[44] Sircar, S. (2002). Pressure Swing Adsorption. *In. Eng. Chem. Res.* Retrieved from https://pubs-acs-org.ezproxy.lib.ucalgary.ca/doi/full/10.1021/ie0109758

[45] Asgari, M., et. al. (2014). Designing a Commercial Scale Pressure Swing Adsorber for Hydrogen Purification. *Petroleum and Coal.* Retrieved from http://www.nitelpars.com/UserImage/article.pdf

[46] Wagner, J. L. (1967). Union Carbide. Selective adsorption process. US Patent No. 3430418A. Retrieved from https://patents.google.com/patent/US3430418A/en

[47] Sircar, S., Golden, T. C. (2000). Purification of Hydrogen by Pressure Swing Adsorption. Retrieved from https://www-tandfonline-com.ezproxy.lib.ucalgary.ca/doi/pdf/10.1081/SS-100100183?needAccess=true

[48] Elseviers, W., et. al. (2015). Honeywell UOP: 50 Years of PSA Technology for H_2 Purification. Retrieved from https://www.uop.com/?document=psa-50-paper&download=1

[49] Ribeiro, A., et. al. (2010). PSA design for stoichiometric adjustment of bio-syngas for methanol production and co-capture of carbon dioxide. *Chem. Eng. Journal.*

[50] Grande, C. (2012). Advances in Pressure Swing Adsorption for Gas Separation. Retrieved from https://www.hindawi.com/journals/isrn/2012/982934/

[51] Petroleum Refining, Volume 2 – Separation Processes. Chapter 10.

[52] Yavary, M., et. al. (2016). Competitive Adsorption Equilibrium Isotherms of CO, CO_2, CH_4, and H_2 on Activated Carbon and Zeolite 5A for Hydrogen Purification. *Journal of Chemical and Engineering Data.*

[53] Remesat, D. (2019). Suncor, Calgary, AB, Canada. In class presentation, University of Calgary, February 2019.

[54] Svrcek, W. Y., Monnery, W. D. (1993). Design Two-Phase Separators Within the Right Limits. *Fluids/Solids Handling*.

[55] (2007). *Standards of the tubular exchanger manufactures association ninth edition*. New York: TEMA.

[56] Towler, G. and Sinnott, R. (2013). *Chemical engineering design*. Oxford: Butterworth-Heinemann.

[57] Couper, J., Penny, W., and Fair, J. (2012). *Chemical Process Equipment: Selection and Design*. Elsevier Science & Technology.

[58] Sinnott, R.K. (1999). *Coulson and Richardson's Chemical Engineering, Volume VI (3rd Edn.).* Butterworth-Heinemann, Oxford.

[59] Menon, S.E. (2004). *Piping Calculations Manual* (1st Edn.). McGraw Hill-Education.

[60] Richard Turton: Analysis Synthesis and Design of Chemical Processes 5th Edition. (n.d.). Retrieved from https://richardturton.faculty.wvu.edu/publications/analysis-synthesis-and-design-of-chemical-processes-5th-edition.

[61] AACE International Certification Programs. (2004). *Project and Cost Engineers Handbook, Fourth Edition Cost Engineering*, 275–284. doi: 10.1201/9780849390388.axa

[62] Dysert, L. R. (n.d.). Cost Estimating Services - Sharpen Your Cost Estimating Skills. Retrieved from https://www.ccg-estimating.com/.

[63] Bradley, D. (2015, August 28). Methanol Prices Face Economic Headwinds, Fitch Says. Retrieved from https://www.naturalgasintel.com/articles/103477-methanol-prices-face-economic-headwinds-fitch-says.

[64] For now, optimism is hard to find in Western Canada's natural gas business | CBC News. (2019, January 2). Retrieved from https://www.cbc.ca/news/business/aeco-alberta-shell-natural-gas-prices-1.4953884.

[65] McShea, W. and Shaw, J. (1982). Method of methanol production, US4927857A.

[66] Cheng, W. and Kung, H. (1994). *Methanol production and use*. New York: Dekker.

[67] Roustapisheh, M. Chemical Engineering Department, University of Calgary, Calgary, AB, Canada. Personal communication, March 2019.